THE JOURNAL OF BIOLOGICAL CHEMISTRY
Vol. 279, No. 31, Issue of July 30, pp. 32474–32482, 2004
Printed in U.S.A.

A Homolog of Prokaryotic Thiol Disulfide Transporter CcdA Is Required for the Assembly of the Cytochrome b_6f Complex in *Arabidopsis* Chloroplasts*[S]

Received for publication, April 19, 2004, and in revised form, May 18, 2004
Published, JBC Papers in Press, May 24, 2004, DOI 10.1074/jbc.M404285200

M. L. Dudley Page‡§, Patrice P. Hamel‡§¶, Stéphane T. Gabilly‡, Hicham Zegzouti‖, John V. Perea, José M. Alonso‡‡, Joseph R. Ecker‡‡, Steven M. Theg**, Sioux K. Christensen‖, and Sabeeha Merchant‡§§**

*From the ‡Department of Chemistry and Biochemistry and the ‖Department of Molecular, Cell, and Developmental Biology, UCLA, Los Angeles, California 90095, the **Division of Biological Sciences, Section of Plant Biology, University of California, Davis, California 95616, and the ‡‡Genomic Analysis Laboratory, The Salk Institute for Biological Studies, La Jolla, California 92037*

The *c*-type cytochromes are defined by the occurrence of heme covalently linked to the polypeptide via thioether bonds between heme and the cysteine sulfhydryls in the C*XX*CH motif of apocytochrome. Maintenance of apocytochrome sulfhydryls in a reduced state is a prerequisite for covalent ligation of heme to the C*XX*CH motif. In bacteria, a thiol disulfide transporter and a thioredoxin are two components in a thio-reduction pathway involved in *c*-type cytochrome assembly. We have identified in photosynthetic eukaryotes nucleus-encoded homologs of a prokaryotic thiol disulfide transporter, CcdA, which all display an N-terminal extension with respect to their bacterial counterparts. The extension of *Arabidopsis* CCDA functions as a targeting sequence, suggesting a plastid site of action for CCDA in eukaryotes. Using PhoA and LacZ as topological reporters, we established that *Arabidopsis* CCDA is a polytopic protein with within-membrane strictly conserved cysteine residues. Insertional mutants in the *Arabidopsis CCDA* gene were identified, and loss-of-function alleles were shown to impair photosynthesis because of a defect in cytochrome b_6f accumulation, which we attribute to a block in the maturation of holocytochrome *f*, whose heme binding domain resides in the thylakoid lumen. We postulate that plastid cytochrome *c* maturation requires *CCDA*, thioredoxin HCF164, and other molecules in a membrane-associated trans-thylakoid thiol-reducing pathway.

The *c*-type cytochromes are a virtually ubiquitous yet rather structurally diverse group of hemoproteins that reside on the so-called *p*-side[1] of the energy-transducing membrane systems where they function typically as electron carriers (1, 2). The *c*-type cytochromes are defined by the occurrence of heme covalently attached to the polypeptide via two thioether linkages between the vinyl groups of heme and the cysteine sulfhydryls in the apocytochrome (1, 3). A C*XX*CH[2] sequence in the apocytochrome provides the thiols for formation of the thioether bonds, and the imidazole of the histidine residue serves as one of the axial ligands of the heme. Remarkably, three distinct assembly pathways, referred to as systems I, II, and III, have emerged through genetic analysis of *c*-type cytochrome maturation in bacteria, chloroplasts, and mitochondria (for review, see Refs. 1 and 4–7), an unexpected finding for what appears on the surface to be a rather simple chemical reaction (*i.e.* the addition of apocytochrome cysteine thiols to the vinyls of heme). Each system can be distinguished on the basis of a sequence relationship of specific assembly factors. Yet, there is an underlying assumption that the three systems are united by common biochemical requirements for holocytochrome *c* biogenesis (for review, see Refs. 2, 4, and 8). For instance, the need for reducing conditions appears to be inherent to the chemistry of thioether bond formation (4). Both substrates, apocytochrome *c* sulfhydryls and heme, need to be maintained reduced prior to the ligation of heme as indicated from *in vitro* and *in organello* experiments (for review, see Refs. 4 and 9).

In bacteria, *c*-type cytochromes are assembled in the periplasm via system I or system II (10, 11). In the bacterial periplasm, a disulfide bond formation machinery (Dsb system in Gram-negative and Bdb system in Gram-positive) promotes the oxidative folding of proteins, which is counter to the requirement for apocytochrome cysteinyl thiols in the heme attachment reaction (12, 13). The current thinking is that apocytochromes *c* upon translocation to the *p*-side are first a substrate of the Dsb/Bdb system which introduces intramolecular disulfides between the two cysteines of the C*XX*CH sequence. Subsequently, the disulfide bond undergoes reduction to provide free sulfhydryls that are competent to react with heme.

The requirement for redox chemistry in the context of *in vivo* cytochrome *c* assembly was appreciated through the discovery

* This research was supported in part by United States Department of Agriculture Grant 98-35306-6975 (to S. M.), National Institutes of Health Grants GM48350 (to S. M.) and GM64584 (to S. K. C.), and by the National Science Foundation (to S. M. T.). The costs of publication of this article were defrayed in part by the payment of page charges. This article must therefore be hereby marked "*advertisement*" in accordance with 18 U.S.C. Section 1734 solely to indicate this fact.

[S] The on-line version of this article (available at http://www.jbc.org) contains an additional Table I and Figs. 1–3 and supplemental experimental procedures.

§ These authors contributed equally to this work.

¶ Supported in part by American Heart Association Fellowship 0120100Y and the Muscular Dystrophy Association Fellowship 3618.

§§ To whom correspondence should be addressed: Dept. of Chemistry and Biochemistry, UCLA, Box 951569, Los Angeles, CA 90095-1569. Tel.: 310-825-8300; Fax: 310-206-1035; E-mail: merchant@chem.ucla.edu.

[1] The *p*-side (for positive) corresponds to the plastid lumen, mitochondrial intermembrane space, or bacterial periplasm. The *n*-side (for negative) is the plastid stroma, mitochondrial matrix, or the bacterial cytoplasm.

[2] The single letter amino acid code is used where *X* is any amino acid except cysteine.

in bacteria of thiol-metabolizing components in systems I and II that constitute a transmembrane thio-reduction pathway (12–14). The components of this pathway include a sulfhydryl-disulfide membrane transporter that conveys reducing power from the cytoplasm to the periplasmic space and a dedicated membrane-anchored thioredoxin that reduces the heme binding site of apocytochrome *c* prior to the heme attachment (13–15).

Plastid *c*-type cytochromes are assembled through system II (5, 16–21), but the requirement for redox chemistry in cytochrome maturation has remained so far largely unexplored in this organelle. We suspected the operation of a redox subpathway in the plastid cytochrome assembly based on the occurrence of a CcdA homolog encoded in the plastid genome of a red alga, *Porphyra purpurea*, and in the nuclear genomes of green alga *Chlamydomonas reinhardtii* and vascular plant *Arabidopsis thaliana.* CcdA is related to the DsbD/DipZ family of membrane polytopic proteins (22) that functions in transmembrane transfer of thiol-reducing equivalents from the bacterial cytoplasm to the periplasm (12, 13, 23). Loss-of-function of CcdA in bacteria results in a pleiotropic deficiency in *c*-type cytochromes, presumably because of a block in the reduction of apocytochrome *c* thiols in the heme binding site (24–28). Interestingly, CcdA is physically linked to a gene encoding a homolog of Ccs1, a system II-specific cytochrome *c* biogenesis (19) in *P. purpurea*, *Mycobacterium* spp., and several cyanobacteria (6). This gene clustering speaks to a role for CcdA in the plastid cytochrome *c* maturation pathway, but no biochemical or genetic evidence is presently available to assign a function to the plant or cyanobacterial CcdAs.

In this work, we investigated the function of *Arabidopsis* CCDA in plastid cytochrome *c* assembly. *In vitro* import experiments and topological analysis using PhoA and LacZ established that the CCDA polypeptide is a polytopic membrane protein that is targeted to the plastid organelle. We have isolated T-DNA and *Ds* (dissociation) element insertions in the *CCDA* gene and shown that loss-of-function alleles resulted in photosynthetic incompetence at the level of cytochrome b_6f assembly. We propose that impaired accumulation of cytochrome b_6f is a consequence of a defect in holocytochrome *f* maturation, a *c*-type cytochrome resident in the plastid lumen. We hypothesize that CCDA is a component of a thylakoid transmembrane thioreduction pathway that operates in the delivery of reducing equivalents to apocytochrome *f* prior to its conversion to the holoform.

EXPERIMENTAL PROCEDURES

Bacterial Strains and Molecular Biology Techniques—Bacterial strain *Escherichia coli* XL1-Blue and DH5-α were used as hosts for recombinant techniques. Strain LMG194 (*phoA*$^-$) was used to measure PhoA activity of the sandwich constructs, and strain CC118 (*phoA*$^-$ *lacZ*$^-$) was used to measure PhoA and LacZ activities. The sources of DNAs used in this work are provided in the on-line supplement.

Constructs for Chloroplast Import Experiments—The AtCCDA, N-AtCCDA-DHFR,[3] and N-AtPC-DHFR constructions were designed in the pGEM2 vector. AtCCDA corresponds to the entire ORF of the *CCDA* gene. N-AtCCDA-DHFR expresses the first 141 amino acids of *Arabidopsis* CCDA fused to the entire coding sequence of the mouse DHFR. N-AtPC-DHFR was engineered by fusing the sequence encoding the 77 amino acids of the plastocyanin chloroplast-targeting sequence plus the first 5 residues of the mature protein to the DHFR sequence. All gene fusions were under the control of the SP6 promoter that enables *in vitro* transcription. The details of the molecular cloning are described in the supplemental material.

Chloroplast Import Experiments—In vitro protein import reactions were performed with chloroplasts isolated from pea seedlings (29). Radiolabeled proteins were translated in wheat germ extract (Promega). Reactions were performed in the light for 20 min prior to thermolysin treatment (29).

Construction of CCDA-phoA, CCDA-lacZ, and CCDA-phoA Sandwich Fusions—Plasmid pRGK200 (30) was used to generate seven *CCDA-phoA* and seven *CCDA-lacZ* translational fusions (I–VII) by a PCR-based strategy. The *phoA* sandwich fusion approach consists of the design of fusion proteins where PhoA is inserted into an otherwise intact target protein (31). Two *CCDA-phoA* sandwich fusions carrying an insertion of *phoA* into *CCDA* at position 202 (SW_A) or 242 (SW_B) of the CCDA protein were constructed in the expression vector pBAD22, a plasmid that harbors an arabinose-inducible *phoA* gene (32). The details of the molecular cloning are provided in the supplemental material.

Measurement of PhoA and LacZ Activities—PhoA assays were performed as described previously in (33), except that isopropyl-1-thio-β-D-galactopyranoside was not used for induction. LacZ activity was measured as detailed in Ref. 34. PhoA assays of the sandwich fusions were performed on overnight grown cultures supplemented with 100 μM L-arabinose for induction. PhoA activity expressed in Miller units was calculated using Equation 1,

$$\text{PhoA activity} = (1{,}000 * A_{420\,nm})/(t * A_{600\,nm}) \quad \text{(Eq. 1)}$$

where *t* is time in minutes. LacZ activity is expressed in units and was calculated by Equation 2,

$$\text{LacZ activity} = (1{,}000 * (A_{420\,nm} - (1.75 * A_{550\,nm}))/(t * A_{600\,nm}) \quad \text{(Eq. 2)}$$

where *t* is time in minutes.

Growth of A. thaliana—Col-0 seeds originated from Lehle Seeds, Round Rock, TX. Plants were propagated on solid minimal media comprising either the commercial soluble fertilizer Peters Professional General Purpose 20-10-20 (35) (Western Farm Services) or 0.5× Murashige & Skoog (MS) minimal medium, solidified with 0.8% (w/v) Select agar (Invitrogen), and containing 0.5 or 5% sucrose, or on a soil mix (Sunshine Professional Basic Mix 2; Sun Gro, Canada). Plants were grown at 24 ± 0.5 °C under white light (80–120 μE/m^2/s) with a light/dark cycle of 16/8 h.

Extraction of Plant Genomic DNA and mRNAs—A. thaliana genomic DNA for Southern hybridization was prepared as described in Ref. 36, except that plant material was frozen in liquid nitrogen and ground to a powder prior to extraction. For PCR amplification, genomic DNAs were extracted as in Ref. 37. Total RNA from plants was isolated with an RNeasy Plant Mini Kit (Qiagen) starting from 100 mg of plant tissue according to the manufacturer's procedure. Following the elution step, purified RNAs were treated for 1 h with RNase-free DNase (Stratagene) to remove any contaminating genomic DNA and phenol-chloroform extracted. To confirm the absence of any contaminating DNA, 50 ng of RNA was subjected to a PCR amplification using the same primers that were used in the RT-PCR analysis.

PCR and RT-PCR Amplifications—PCR amplifications performed as part of the University of Wisconsin-Madison screening process were carried out using TAKARA Ex-Taq under the conditions recommended by the manufacturer. The reverse transcription reaction was performed using the RT system (Promega); see the supplemental material.

Screening and Molecular Characterization of ccda Mutant Lines—The PCR-based service provided by the *Arabidopsis* Knockout Facility at the University of Wisconsin-Madison Biotechnology Center was used to screen 60,480 T-DNA insertion lines, and one insertion in the *CCDA* gene was identified (*ccda-1*). The ET5250 line carrying a *Ds* element insertion (*ccda-2*), the SALK_025766 line (*ccda-3*) and SALK_014416 line (*ccda-4*), both harboring a T-DNA insertion in *CCDA*, were identified through querying data bases of sequenced insertion sites (Cold Spring Harbor laboratory and Salk Institute Genomic Analysis Laboratory, respectively). The details of the screening and molecular characterization of the mutant lines are available in the supplemental material.

Fluorescence Measurements—The fluorescence imaging system, Fluorcam 700 MF (Photon Systems Instruments Ltd.), was used to record chlorophyll fluorescence induction and decay kinetics of *Arabidopsis* plants that had been dark-adapted for at least 5 min. Plants were illuminated for 20 s under actinic light of 50 μE/m^2/s. Emitted fluorescence was captured by the camera, and the collected data were converted into a graph using Excel software (Microsoft).

Protein Preparation and Analysis—To extract proteins, plant tissue was frozen in liquid nitrogen, ground to a powder, and ground further in ice-cold extraction buffer (50 mM Tris-HCl, pH 8.0, 5 mM EDTA). The

[3] The abbreviations used are: DHFR, dihydrofolate reductase; kan^r, kanamycin-resistant; kan^s, kanamycin-sensitive; MS medium, Murashige & Skoog medium; ORF, open reading frame; RT, reverse transcription.

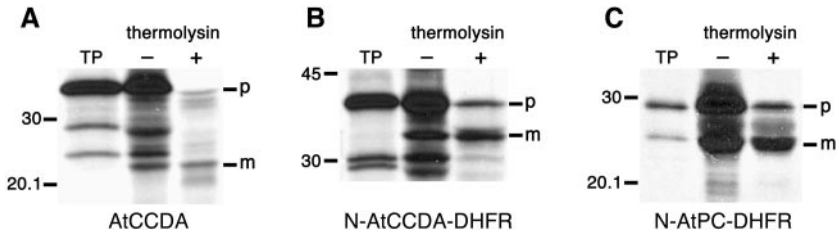

FIG. 1. **The N terminus of *Arabidopsis* CCDA contains a chloroplast transit peptide.** *A*, pre-CCDA is imported into plastids and processed to a mature form. *B* and *C*, import of DHFR chimeras containing the N termini of the precursors of CCDA and plastocyanin (*PC*), respectively. Protein import reactions were performed as described under "Experimental Procedures"; the resulting fluorographs are shown. DHFR import driven by a known targeting sequence (AtPC) from preapoplastocyanin is shown for comparison (*C*). *Lanes* marked *TP* were loaded with translation product equivalent to 20% of that run in the import reaction; *lanes* marked + and − refer to the postreaction addition (or not) of thermolysin; *p* and *m* mark the positions of the precursor and mature forms of the translated proteins, and the positions of molecular mass markers are indicated as kDa on the *left* of each gel: AtCCDA (40 kDa) N-AtCCDA-DHFR (36.5 kDa), and N-AtPC-DHFR (29.5 kDa) run as expected from their calculated molecular masses.

homogenates were centrifuged at 13,000 × *g* for 15 min at 4 °C, and the pellets, enriched in membrane proteins, were washed twice and resuspended in extraction buffer (0.5–2.0 ml/g of fresh tissue). Protein concentration was determined using the bicinchoninic acid assay (38). In-gel heme stain of holocytochome *f* was performed using TMBZ (39). Immunoblotting of proteins separated by SDS-PAGE was performed as in Ref. 40, except that samples were heated at 37 °C for 30 min. Antibody dilutions were 1:1,000 for anti-CF_1 (spinach), anti-Cox1, anti-cyt *f*, anti-subunit IV/PetD (*C. reinhardtii*), and anti-HCF164 (*A. thaliana*); 1:2,000 for anti-Sec12 (*A. thaliana*) and anti-cyt b_6 (*C. reinhardtii*); and 1:3,000 for anti-Rieske FeS (maize). A 1:3,000 dilution of alkaline phosphatase-conjugated goat anti-rabbit IgG was used as the secondary antibody. Sample loading was adjusted so that each sample contained the same amount of the α subunit of CF_1. Quantitation of the bands was performed using a MultiImage system running ChemImager 4400 software (Alpha Innotec).

RESULTS

A Homolog of Prokaryotic Thiol Disulfide Transporter CcdA in Photosynthetic Eukaryotes—We had noted the occurrence of a CcdA-encoding gene in the plastid genome of a rhodophyte alga, *P. purpurea* and also in the genomes of several cyanobacteria (6). With red algal CcdA as our prototype, we searched the nucleotide sequence data bases and identified expressed sequence tags corresponding to CcdA-like proteins from a number of photosynthetic eukaryotes, including *Chlamydomonas*, *Arabidopsis*, and several other vascular plants.[4] A full-length cDNA was identified for each and sequenced.[5] A multiple alignment of the conceptual protein sequences (see Fig. 1 in the supplemental data) confirmed that the two cysteines that are essential for the redox activity of bacterial CcdA (26) are invariant in the plant homologs and revealed that all display an N-terminal extension relative to the plastid-encoded and prokaryotic CcdA proteins, suggesting plastid localization of the nucleus-encoded plant homologs. All eukaryotic CCDAs displayed the features of polytopic membrane proteins with six predicted transmembrane segments when analyzed *in silico* for the presence of hydrophobic domains (Fig. 1 in the supplemental data). To assess the function of plant CCDA, three specific questions were addressed: 1) Where is CCDA localized? 2) What is its topological arrangement? and 3) What is the phenotype of loss-of-function *ccda* plants?

Arabidopsis CCDA Is Targeted to the Plastid—The direct approach of immunolocalizing CCDA polypeptide after cell fractionation was not successful because the antisera we raised reacted very weakly if at all with native CCDA, perhaps because it is a low abundance hydrophobic protein (data not shown). Therefore, we chose to localize the *in vitro* synthesized radiolabeled protein after *in vitro* import into pea chloroplasts. We certainly expected CCDA to localize to chloroplasts based on the occurrence of the gene in the less derived red algal plastid genome of *P. purpurea* (6). Indeed, AtCCDA could be imported into isolated chloroplasts and was processed to the mature form, suggesting that the N-terminal extension functions as a chloroplast-targeting presequence *in vitro* (Fig. 1*A*). We further solidified this model by showing that the 141-amino acid N-terminal extension on CCDA could target a passenger protein like the widely used reporter, DHFR, to the chloroplast *in vitro* (Fig. 1*B*). As a positive control for import, we used the 77-amino acid targeting sequence of plastocyanin, a known thylakoid lumen resident protein. As expected, the targeting sequence of plastocyanin is able to drive import of DHFR into the chloroplast (Fig. 1*C*). We concluded that CCDA is targeted to the chloroplast via its N-terminal extension and that its plastid location is compatible with a function in chloroplast cytochrome *c* biogenesis.

Plastid CCDA Is a Polytopic Membrane Protein with Within-membrane Invariant Cysteines—To verify experimentally the predicted six-transmembrane segment model for chloroplast CCDA and, in particular, to locate the two universally conserved cysteines, we used PhoA and LacZ as topological reporters in bacteria. This approach relies on the topological analogy in a bioenergetic sense between the *p*-side and *n*-side compartments in bacteria (periplasm/cytoplasm) and those in plastids (lumen/stroma) and is justified by the previous establishment of its reliability for the analysis of CcsA, a thylakoid membrane polytopic protein (21). Translational fusions between CCDA and PhoA or LacZ were engineered at predicted periplasmic and cytoplasmic loops. The topology was deduced on the basis of measured LacZ and PhoA activities of the fusions proteins expressed in *E. coli* (Fig. 2 and Table I). High PhoA activities indicate a *p*-side location for the insertion site of the fusion because PhoA is active only in the periplasm. Reciprocally, fusions with high LacZ activity confirm association of the α and ω fragments of LacZ in the cytoplasm, and therefore an *n*-side location of the fusion site can be deduced. Location of the third extramembrane loop to the *n*-side or the *p*-side of the membrane could not be ascertained because both CCDA-PhoA and CCDA-LacZ fusions at position 236 of the polypeptide display high enzymatic activity (Table I, see fusion IV). We have ruled out that this is the result of a position effect at this particular site because fusions at positions 243, 249, and 254 in CCDA, all predicted to be located on the *n*-side, also led to high PhoA activity (data not shown). To overcome the ambiguity concerning the location of the third loop, we exploited the so-called sandwich approach, which offers greater reliability for examining membrane protein topology (31). In this method, PhoA is

[4] *Descurainia sophia*, *Glycine max*, *Hordeum vulgare*, *Lotus japonicus*, and *Medicago truncatula* (TBLASTN scores ranged from 10^{-17} to 10^{-55}).

[5] GenBank™ accession numbers: *C. reinhardtii*, AAL84598; *A. thaliana*, AAF35369; *D. sophia*, AAQ95739; *G. max*, AAP81162; *H. vulgare*, AAO16019; *L. japonicus*, AAO16018; and *M. truncatula*, AAO16020.

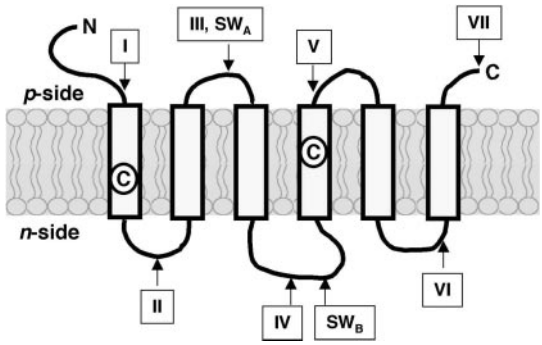

FIG. 2. **Topological model of *Arabidopsis* CCDA.** The topological arrangement of *Arabidopsis* CCDA in the thylakoid membrane was deduced according to PhoA/LacZ fusion analysis in bacteria (Table I). The *p*-side corresponds to the lumen of the thylakoid, and the *n*-side corresponds to the stroma of the chloroplast. The transmembrane helices of CCDA as predicted from *in silico* analysis (67) are represented by *gray rectangles* within the lipid bilayer. *Thick lines* feature extramembranous regions of the CCDA polypeptide. The *arrows* indicate, within CCDA, the positions of in-frame alkaline phosphatase and β-galactosidase fusions. Fusions at positions 107 (I), 181 (II), 202 (III and SW$_A$), 236 (IV), 242 (SW$_B$), 277 (V), 322 (VI), and 353 (VII) are indicated on the drawing by *arrows*. Strictly conserved cysteine residues that lie within the membrane are marked *C*.

TABLE I
CCDA-PhoA and -LacZ activities

Alkaline phosphatase and β-galactosidase activities of CCDA fusion proteins expressed in bacteria were measured as described under "Experimental Procedures." At least two representatives of each CCDA fusion that was generated by PCR were tested for activity. PhoA activities (Miller units) and LacZ activities (A.U.) values are the means of three independent measurements. *n*-side and *p*-side correspond to the negative and positive sides of the membrane, respectively. NA, not applicable.

	PhoA activity	LacZ activity	Topology
	Miller units	*units*	
I	218 ± 20	59 ± 20	*p*-side
II	55 ± 8	1224 ± 149	*n*-side
III	1468 ± 142	16 ± 5	*p*-side
IV	289 ± 76	14,520 ± 400	?
V	888 ± 37	<0.01	*p*-side
VI	<0.05	12,821 ± 1,766	*n*-side
VII	212 ± 38	<0.01	*p*-side
SW$_A$	344 ± 11	NA	*p*-side
SW$_B$	10 ± 1	NA	*n*-side

inserted in an otherwise intact CCDA protein (see *arrows* marked *SW* in Fig. 2). The measurement of PhoA activity of sandwich constructs SW$_A$ and SW$_B$ yielded a definitive placement of the third loop to the stromal *n*-side (Table I). Using an anti-PhoA antibody, we were able to detect the CCDA-PhoA sandwich protein in the membrane fraction of bacterial cells expressing the SW$_A$ construct (data not show). We could not detect the CCDA-PhoA sandwich protein expressed from the SW$_B$ construct, suggesting that the protein is not stable and undergoes degradation. This has been observed for fusion proteins where the cytoplasmic form of the alkaline phosphatase often fails to fold into a stable structure (26, 41). The experimentally deduced model is in agreement with the topological prediction and consists of a six-transmembrane protein with N and C termini on the lumen side.

Identification of Mutants with T-DNA and Ds Element Insertions in the CCDA Gene—To assess plant CCDA function, we sought next to take a reverse genetic approach. This was facilitated by the possibility to screen for T-DNA inserts in genes of interest in *Arabidopsis* (42, 43) and to obtain mutant lines from publicly available library stocks. Four candidate *ccda* mutant

TABLE II
T-DNA and Ds element integration sites in A. thaliana mutant lines

Underlining indicates the 8 bp of *A. thaliana* DNA duplication accompanying the insertion of *Ds* element in the *CCDA* gene. **ATG-** marks the *CCDA* start codon. ▼ indicates the position of the integrated DNA, and Δ (bp) shows the size of the deletion of *A. thaliana* genomic DNA upon integration of the interrupting element.

ccda-1 –TTTATATACTTGT—▼—TTCAATTATGTTC–
Δ 36 bp
ccda-2 –CGCTTATCTGGAAG-▼-TCTGGAAGGAGAGTC**ATG**—
ccda-3 –TTAATGGGC—▼—GACGCTTATCTGGAAGGAGAGTC**ATG**–
Δ 98 bp
ccda-4 –GGGTTCGTGCTGG—▼—GAGAGGGAGAGA–
Δ 16 bp

lines corresponding to one enhancer trap line with a *Ds* element (44) and three T-DNA lines (43) were identified experimentally by screening pooled genomic DNAs (42) at the PCR-based *Arabidopsis* Knockout Facility or by querying data bases of sequenced insertion sites. The exact positions of the insertion sites of the T-DNAs and the *Ds* elements were determined by sequencing PCR products encompassing the genomic border of the integration site (Table II). The *Ds* element insertion site in allele *ccda-2* is in the 5′-untranslated region of the *CCDA* gene, 15 bp upstream from the putative start codon (Fig. 3 and Table II). The three T-DNA insertion sites mapped to the 5′-untranslated region, 23 bp upstream from the start codon (*ccda-3* allele), to exon II (*ccda-4* allele) and to intron III (*ccda-1* allele) of the *CCDA* gene (Fig. 3 and Table II).

Plants hemizygous for insertions at the *CCDA* locus were generated and self-fertilized to monitor Mendelian transmission of the interrupting elements. This was achieved by scoring phenotypically for kanamycin resistance conferred by the *nptII* marker present on the T-DNA and *Ds* elements and molecularly by DNA hybridization analyses (see "Experimental Procedures" and Fig. 2 in the supplemental data).

The progeny arising from self-fertilization of the heterozygous *ccda-1* plant exhibited a kan^r:kan^s ratio of 322:17, or ~15:1, suggesting the presence of two segregating T-DNA insertions/genome. This was confirmed by Southern hybridization (Fig. 2*A* in the supplemental data), and heterozygous plants carrying only the *ccda*-inserted T-DNA were identified (Fig. 2*A* in the supplemental data). These were grown to maturity and allowed to self-pollinate to generate the *ccda-1* homozygous line.

The progeny of self-fertilized *CCDA*/*ccda-4* plants exhibited a kan^r:kan^s ratio of 72:26, or ~3:1, suggesting the presence of a single segregating T-DNA/genome. This was confirmed by Southern hybridization (Fig. 2*B* in the supplemental data). The progeny of self-fertilized *CCDA*/*ccda-2* and *CCDA*/*ccda-3* plants exhibited kan^r:kan^s ratios of ~3:1 and 15:1, indicative of the segregation of one single *Ds* element and two T-DNA elements, respectively. Preliminary characterization revealed that plants homozygous for *ccda-2* and *ccda-3* alleles could be grown to maturity on soil (see below), and further clean-up of the *ccda-3* allele carrying line was omitted.

The molecular arrangement of each insertion in the *CCDA* gene was analyzed by PCR using T-DNA/*Ds*-specific and *CCDA*-specific primers (see supplemental material). This analysis indicated that the T-DNA insertions in *ccda-1*, *ccda-3*, and *ccda-4* are all tandem or complex insertions carrying two left borders at their extremities (45). In the case of the *ccda-2* allele, the simplest interpretation is the integration of a single *Ds* element (Fig. 3 and Fig. 3 in the supplemental data).

Growth Characteristics and Fluorescence Transients of the ccda Mutant Lines—Because loss of CCDA function is anticipated to block assembly of plastid *c*-type cytochrome, holocytochrome *f*, and consequently impair photosynthesis, homozy-

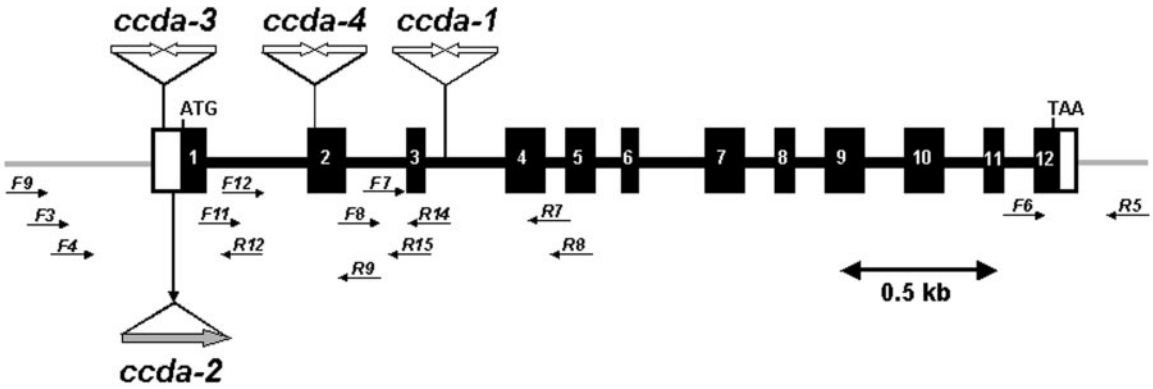

FIG. 3. ***Arabidopsis CCDA* genomic locus.** The genomic locus of *Arabidopsis CCDA* is drawn as a *thick line* and includes 12 exons (*numbered black boxes*) and 11 introns. Genomic DNA flanking the *CCDA* locus is drawn as a *gray line*. *ATG* and *TAA* indicate initiation and stop codon of *CCDA* ORF, respectively. The insertions of an interrupting element are indicated as *gray* (*Ds*) or *white* (T-DNA) *arrows*. The directionality of the interrupting element is indicated by the orientation of the *arrow* (*left border* → *right border* for the T-DNA and 5′ → 3′ for the *Ds* element). Primers used for molecular characterization of the *ccda* alleles are drawn as *thin arrows*.

gous *ccda*-interrupted plants were examined at the level of growth and photosynthetic electron transfer by recording chlorophyll fluorescence induction and decay kinetics. For fluorescence measurements, plants were propagated as segregating populations on MS medium containing 0.5% sucrose, and each plant was subsequently genotyped by PCR to identify *ccda* homozygotes. Plants homozygous for either the *ccda-2* or the *ccda-3* allele were phenotypically indistinguishable from wild type lines (data not shown). The plants grew on soil, flowered, set seeds normally, and behaved as their corresponding wild type with respect to photosynthetic electron transfer (data not shown). Homozygotes for the *ccda-1* allele grew very slowly on soil and remained pale green (Fig. 4 and not shown), but after 60 days the plants, although quite small, produced a few flowers and set seeds. Consistent with the growth defect, mutant plants displayed a leaky *hcf* (high chlorophyll fluorescence) phenotype (Fig. 4) typical of photosynthetic mutants that are not completely blocked in the function of the b_6f complex (46). Of 77 plants analyzed in the segregating population, 63 exhibited wild type fluorescence and 14 a *hcf* phenotype, making a ~3:1 ratio ($\chi^2 = 1.06$). That the *hcf* phenotype cosegregated with the *ccda-1* genotype suggested that the T-DNA integration in *CCDA* was responsible for the lesion we observed. Mutants homozygous for *ccda-4* were seedling-lethal (not shown) and could only grow on a minimal synthetic medium supplemented with 0.5% sucrose, as expected for photosynthesis-minus *Arabidopsis* plants (46). The *ccda-4* homozygous plantlets obtained on 0.5% sucrose-containing medium were about half the size of the wild type and heterozygous segregants grown in the same conditions (not shown). They displayed a tight *hcf* phenotype consistent with a complete loss of the cytochrome b_6f complex and hence photosynthetic growth (Fig. 4). Of 167 plants examined among the segregants, 131 exhibited wild type fluorescence and growth and 36 a *hcf* and reduced growth phenotype. This 3:1 distribution ($\chi^2 = 0.554$) and the fact that the *hcf* phenotype cosegregated with the *ccda-4* genotype suggested that the observed phenotype is attributable to the T-DNA integration. Interestingly, growth in the presence of 5% sucrose resulted in *ccda-4* homozygous plants that were similar in size to the corresponding wild-type and heterozygous segregants but which produced only a few small flowers that did not fully open (data not shown).

The direct correlation between the photosynthetic phenotype of the *ccda* mutant lines and the severity of the molecular lesions suggest that the level of expression of the *CCDA* gene product is directly responsible for the observed phenotype.

Analysis of CCDA Transcripts in ccda Mutant Lines—We monitored the level of expression of the *CCDA* gene in the different mutant lines by RT-PCR analysis. As shown in Fig. 5*A*, both *ccda-2* and *ccda-3* homozygous lines that display no visible phenotype still express the *CCDA* mRNA, suggesting that the insertion of T-DNA or *Ds* elements in the 5′-untranslated region did not abolish the transcriptional activity of the *CCDA* gene. By contrast, plants carrying the *ccda-1* and *ccda-4* mutations that result in impaired photosynthesis do not accumulate the *CCDA* mRNA, and consequently, those mutations correspond to loss-of-function type of alleles. However, the difference in the severity of the photosynthetic phenotypes caused by the *ccda-1* or *ccda-4* alleles suggests that those mutations do not both cause a complete lack of function of the CCDA protein. By RT-PCR, we were able to show that both mutant lines expressed a truncated form of the *CCDA* mRNA (Fig. 5*B*). One possible explanation for the phenotypic differences is that in *ccda-4*, the mRNA does not encode a functional protein, whereas in *ccda-1* the truncated protein still exhibits some activity.

As a control, we showed that the *ccda* mutations do not modify the expression of chloroplast *petA* and *petB* genes encoding apocytochrome *f* and apocytochrome b_6, respectively (Fig. 5*A*).

Mutations in CCDA Result in a Defect in Cytochrome b_6f Complex Accumulation—We assessed the abundance of holocytochrome *f* in the mutant lines by heme staining and immunoblotting and also that of Rieske FeS, cytochrome b_6, and subunit IV, which are subunits of the cytochrome b_6f complex. As expected from the lack of phenotype in the *ccda-2* and *ccda-3* lines, holocytochrome *f* accumulation is not affected by these mutations, and the molecule assembles to essentially wild type level (Fig. 6). By contrast, the *ccda-1* mutation causes a severe reduction in the level of holocytochrome *f*. Only 20–25% of wild type levels of holocytochrome *f* is detected in the *ccda-1* line. Concomitant with the diminution in holocytochrome *f* abundance, we observed a decrease in the accumulation of the subunits of the cytochrome b_6f complex (Fig. 6). The *ccda-4* mutation that leads to a more drastic phenotype than the *ccda-1* mutation has a more pronounced effect on holocytochrome *f* accumulation. Only 10% of wild type level of cytochrome *f* is assembled in this mutant line, and the abundance of cytochrome b_6f subunits is also likewise severely reduced (Fig. 6). We concluded that loss-of-function *ccda* alleles lead to a defect in plastid biogenesis that is the result of impaired accumulation of the cytochrome b_6f complex in the thylakoid membranes.

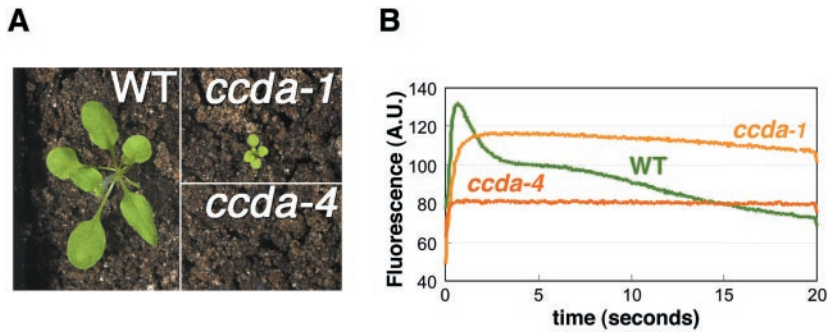

FIG. 4. ***ccda-1* and *ccda-4* homozygous plants are photosynthetically incompetent.** *A*, Col-0 ecotype wild type (*WT*), *ccda-1* and *ccda-4* homozygous plants are shown 20 days after germination on soil. *B*, the fluorescence induction and decay kinetics observed in a dark to light transition for *ccda-1* and *ccda-4* homozygous mutants are shown compared with those of Col-0 ecotype wild type. Ws ecotype wild type fluorescence transient is not shown but was found to be similar to Col-0 wild type. The *continuously rising curve* for the *ccda* mutant is the signature of a specific block in electron transfer at the level of cytochrome b_6f complex because of its impaired assembly in the absence of membrane-bound holocytochrome *f*. When the energy absorbed by the chlorophyll cannot be utilized because of a block in photosynthetic electron transfer, an increase in the chlorophyll fluorescence is observed. Note the absence of the decay phase corresponding to reoxidation of the quinone pool (the primary electron acceptor of photosystem II) by the cytochrome b_6f complex.

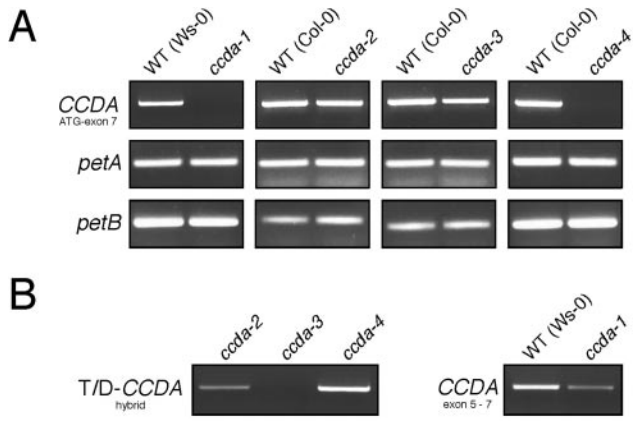

FIG. 5. **Expression of the *CCDA* gene in the *ccda* mutant lines.** RT-PCR experiments were performed as described under "Experimental Procedures." PCR amplification products were separated by agarose gel electrophoresis and visualized after staining with ethidium bromide. *A*, amplification of *CCDA* (from ATG to exon 7), *petA* (cytochrome *f*), and *petB* (cytochrome b_6) transcripts in *ccda* mutant lines and corresponding wild type ecotypes using RT-F12, RT-R4, petA-L, petA-R, and petB-L, petB-R primers, respectively (see Table I supplemental data). *B*, *left*, amplification of T-DNA (*Ds*)/CCDA hybrid transcript in *ccda-3* and *ccda-4* lines using T-DNA-specific RT-LB1 primer and *CCDA*-specific RT-R4 primer and in *ccda-2* line using *Ds* element-specific primer *Ds*-RT1 and *CCDA* primer RT-R4. *Right*, amplification of the 3′-end of the *CCDA* transcript (from exon 5 to exon 7) in the *ccda-1* line and corresponding wild type ecotype with *CCDA*-specific primers RT-F5 and RT-R4 (see Table I supplemental data). The predicted sizes of the PCR products are: *CCDA* (from ATG to exon 7), 672 bp; *petA*, 158 bp; *petB*, 185 bp; *Ds-CCDA* hybrid in *ccda-2*, 697 bp; T-DNA-*CCDA* hybrid in *ccda-3*, 726 bp; T-DNA-*CCDA* hybrid in *ccda-4*, 599 bp, *CCDA* exons 5–7, 209 bp.

DISCUSSION

In an attempt to determine whether a thio-reduction pathway operates in the chloroplast, we have investigated the function of an *Arabidopsis* homolog of the prokaryotic sulfide-disulfide transporter CcdA that is known to function in the analogous pathway in bacteria. In this paper, we provide evidence that *Arabidopsis* CCDA is 1) a chloroplast protein, 2) a polytopic membrane protein with within-membrane cysteine residues and that 3) mutations in the *CCDA* gene lead to a defect in plastid biogenesis associated with a loss in cytochrome b_6f assembly.

Arabidopsis CCDA Is a Chloroplast Polytopic Membrane Protein—All vascular plant CCDA homologs that we identified exhibit an additional stretch of 100–115 amino acids in the N-terminal part of the polypeptide that is missing in the rhodophyte homolog encoded in the plastid genome (see Fig. 1 in the supplemental data). *Chlamydomonas* CCDA displays the shortest N-terminal extension (61 amino acids), a feature that is common to algal transit peptides that are 32 amino acids shorter, on average, than those from vascular plants (47). The N-terminal extensions present typical features of bipartite transit sequences that direct proteins to the thylakoid membrane via the so-called "spontaneous import pathway" (48, 49). The first domain directs the protein across the envelop into the stroma, whereas the second domain carries targeting information to the thylakoid. Both domains in the N-terminal extensions exhibit the expected characteristics: the former is hydrophilic and rich in hydroxylated residues, and the latter contains a positively charged N terminus followed by a hydrophobic segment, which is a crucial determinant for thylakoid translocation and ends with a processing site (AXA↓) for the thylakoid processing peptidase (see Fig. 1 in the supplemental data). Our *in vitro* experiments have established that this N-terminal extension indeed serves as a chloroplast-targeting sequence and is cleaved off upon import as expected for nuclearly encoded proteins that function in the plastid organelle. The sublocalization of CCDA could not be examined by conventional cell fractionation techniques because we were unable to generate an immunoreactive probe for the polypeptide. However, based on the presence of the bipartite chloroplast-targeting sequence and the polytopic model of CCDA that we have generated from PhoA-LacZ fusion analysis, we can deduce indirectly that CCDA is localized to the thylakoid membrane. Our topogical model is compatible with the experimentally deduced topology of bacterial *Rhodobacter capsulatus* CcdA (26), and it is noteworthy that in both plastid and bacterial CcdAs, the critical cysteine residues are assigned a within-membrane location in the first and the fourth transmembrane segments. The exact position of these cysteines, whether embedded or in proximity to the stromal or luminal sides, cannot be resolved by our topological experiments. The function of the within-membrane cysteines in CCDA is not really known, but functional dissection of the related bacterial DsbD/DipZ transporter has demonstrated that the redox active cysteines face the cytoplasmic side of the membrane (50). These cysteines have the potential to form a disulfide bond, an indication of their physical vicinity, and are key residues in the relay of reducing equivalents originating from the cytoplasm (50). It is likely that conserved cysteines in CCDA are also facing the stromal side of the thylakoid membrane and operate in a similar manner.

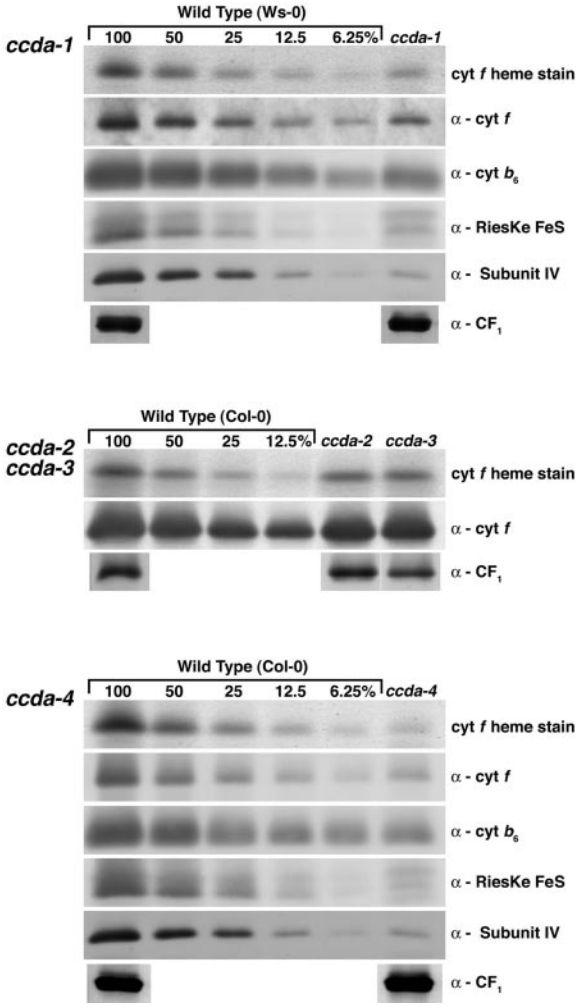

FIG. 6. **Accumulation of cytochrome b_6f subunits in *ccda* mutants.** Protein fractions were prepared from entire wild type (*Ws-0* and *Col-0*) and homozygous *ccda-1*, *ccda-2*, *ccda-3* plants grown on MS medium supplemented with 0.5% sucrose, or from wild type (Col-0) and *ccda-4* grown on MS medium supplemented with 5% sucrose. Samples were loaded on the basis of an equal amount of subunit α of CF_1 and separated by SDS-PAGE (12% acrylamide). For an estimation of the subunit abundance, dilutions of the wild type sample were loaded on the gel. In-gel heme staining of cytochrome *f* was performed using TMBZ (39). Proteins were transferred to nitrocellulose membranes after electrophoresis, and immunodecoration was carried out using antisera against spinach cytochrome *f* and CF_1, *Chlamydomonas* cytochrome b_6 and subunit IV, and maize Rieske FeS. Equal loading of samples was further confirmed by verifying that the abundance of Cox1 (mitochondria) and Sec12 (endoplasmic reticulum) was unchanged in all samples (not shown). The extent of reduction in the protein abundance in *ccda* mutants is different for each subunit (compare, *e.g.* cytochrome b_6 and Rieske FeS) because the steady-state level of each cytochrome b_6f subunit (whether assembled in a complex or unassembled/disassembled in the membrane) reflects its individual rate of synthesis and degradation.

Mutations in CCDA Indicate a Function in the Biogenesis of the Cytochrome b_6f Complex—The severity of the photosynthetic phenotype in the *ccda* lines correlates nicely with the impact of the interrupting DNA elements on the expression of the *CCDA* gene. The two insertions in *ccda-2* and *ccda-3* lines which lie in the 5′-untranslated region of the *CCDA* gene did not result in any observable phenotype under our conditions, either at the level of growth on soil or when examined for the accumulation of the cytochrome b_6f complex. Neither insertion prevented the transcription of the *CCDA* gene, a rather surprising finding considering that the interrupting elements are only 15 and 23 bp away from the initiation codon of the *CCDA* gene. One likely explanation is that both the T-DNA and the *Ds* element harbor some promoter-like activity that enables transcription of *CCDA*. The *Ds* element is known to carry a promoter-like sequence at its 3′-end that can be activated upon integration (51). Indeed, we could detect a hybrid RNA in the *ccda-2* line using a *Ds* element-specific primer and a *CCDA*-specific primer (Fig. 5*B*), confirming that the element does not block expression of *CCDA*. Despite several attempts, a transcript originating from the T-DNA in the *ccda-3* line could not be detected by RT-PCR (Fig. 5*B*). However, based on the observation that the T-DNA in the *ccda-4* line allows transcription of a truncated *CCDA* mRNA (Fig. 5*B*), we assume that the *CCDA* mRNA produced in the *ccda-3* line also originates from the T-DNA. Lack of phenotype because of insertion of interrupting element in proximity to the initiation codon has also been reported previously in *Arabidopsis* (52).

The *ccda-1* and *ccda-4* lines do not express the full-length *CCDA* mRNA and result in photosynthetic incompetence that is correlated to decreased level of assembled cytochrome b_6f complex. The *ccda-1* and *ccda-4* alleles cause distinct phenotypes: the former leads to a partial loss of function with 25% of assembled holocytochrome *f* that enables photosynthetic growth, and the latter results in complete loss of function with only 10% of accumulated holocytochrome *f*, which prevents photosynthetic growth. It is interesting to note that 25% of the level of holocytochrome *f* is sufficient to sustain germination and photosynthetic growth, whereas only 10% of the level of cytochrome *f* is insufficient for photosynthetic growth.

Unexpectedly, truncation of the first three exons in the *ccda-1* allele does not produce a complete knock-out of the *CCDA* gene. Somehow, despite the lack of the first 90 amino acids that carry the targeting information, the truncated protein is still able to function in the assembly of the cytochrome b_6f complex. It is possible that targeting information lies also in the hydrophobic core of the polypeptide or that the N-terminal sequence created by the fusion between the T-DNA and the *CCDA* gene is compatible with import into the thylakoid membrane.

CCDA May Correspond to an Eighth Component in the System II Pathway in Plastid—Our data support the implication of CCDA in a process required for the biogenesis of cytochrome b_6f complex but do not elucidate whether heme attachment to apocytochrome *f* is compromised by *ccda* mutations. The defect in cytochrome b_6f biogenesis in the absence of CCDA is most likely the result of compromised assembly of the complex, consistent with the observation that holocytochrome *f* is required for the assembly of the b_6f complex in *Chlamydomonas* (53). A definite placement of CCDA in the plastid *c*-type cytochrome assembly pathway also relies on the examination of the assembly of cytochrome c_X, the other *c*-type cytochrome occurring in the thylakoid lumen in *Arabidopsis* (54). This was not feasible because of the extraordinarily low abundance of this molecule in the plastid, whose holoform can only be detected in plants engineered to overexpress the protein (55). The green alga *C. reinhardtii* remains the ideal system to study plastid *c*-type cytochrome assembly because of the availability of *ccs* mutants (*c*ytochrome *c* synthesis) that are blocked at the level of heme attachment to the apoforms of cytochrome *f* and cytochrome c_6, the two *c*-type cytochromes resident in the lumen (56–59). Seven loci, plastid *ccsA* and nuclear *CCS1* to *CCS6*, are required for the accumulation of both plastid holocytochrome *f* and c_6 (17, 20).[6] The presence of a CCDA homolog in *Chlamydomonas* prompted us to examine whether unidentified *CCS2* to *CCS6* loci could correspond to the *CCDA* gene. Two cosmids

[6] P. Hamel and S. Merchant, unpublished data.

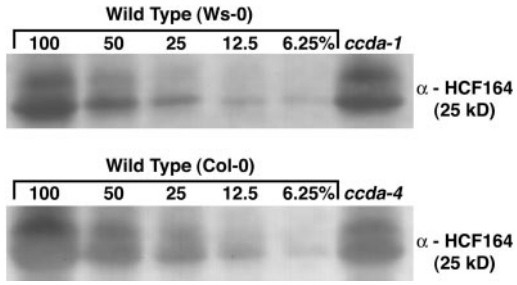

FIG. 7. **Accumulation of HCF164 thioredoxin in *ccda-1* and *ccda-4* mutants.** Protein fractions were prepared from entire wild type (*Ws*) and homozygous *ccda-1* plants grown on MS medium supplemented with 0.5% sucrose and from wild type (*Col-0*) and homozygous *ccda-4* plants grown on MS medium supplemented with 5% sucrose. Samples were normalized for loading on the basis of an equal amount of subunit α of CF_1 and separated by SDS-PAGE (12% acrylamide) to detect HCF164 thioredoxin (62). After electrophoresis, proteins were transferred to nitrocellulose membranes before immunodecoration with *Arabidopsis* anti-HCF164. Equal loading of samples was further confirmed by verifying that the abundance of Cox1 (mitochondria) and Sec12 (endoplasmic reticulum) was unchanged in all samples (not shown).

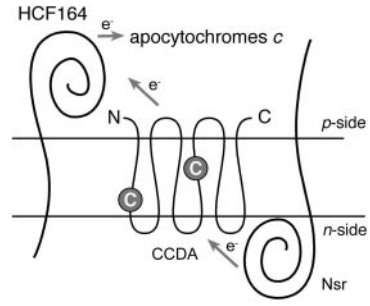

FIG. 8. **Model for a thioreduction pathway in plastid *c*-type cytochrome maturation.** Our current view is that delivery of thiol-reducing equivalents (e^-) from the *n*-side to the *p*-side of the thylakoid membrane is necessary to maintain apocytochrome sulfhydryls in a reduced state prior to heme ligation. This thioreduction pathway includes CCDA and requires additional reaction partners on both sides of the membrane, like *Nsr* for the *n*-side reductant, which could be a membrane-anchored stroma facing thioredoxin, and HCF164, which is a candidate for the *p*-side reductant. The source of reducing power on the stromal side is not known and could be ferredoxin or NAD(P)H as in the bacteria (12, 13).

(p*ARG7-CCDA*) carrying the *ARG7* selection marker and containing genomic DNA[7] corresponding to *Chlamydomonas CCDA* plus 5′- and 3′-flanking DNA were identified. The p*ARG7-CCDA* cosmids were tested directly for their ability to rescue representative mutants corresponding to each of the *CCS2* through *CCS6* loci or indirectly for restoration of photosynthetic growth in arginine prototrophs resulting from transformation of *ccs arg7* mutants. For most strains, we also analyzed the *CCDA* locus physically by blot hybridization and sequence analysis of the entire ORF. Based on the lack of complementation and absence of physical change in the *CCDA* gene in the *ccs* mutants, we concluded that if CcdA is involved in cytochrome *c* biogenesis, then it must correspond to a component that is not yet genetically defined.

There is the formal possibility that plastid CCDA is necessary for other processes controlling the biogenesis of cytochrome b_6f complex, such as, for instance, maturation of the recently discovered covalent heme on holocytochrome b_6 (60, 61). However, a function of CCDA in holocytochrome b_6 assembly seems unlikely based on the fact that the covalent heme in holocytochrome b_6 is on the stromal side (60, 61) and that covalent binding of heme to bacterial holocytochrome *b* is not dependent upon CcdA (25). That CCDA is recruited to complete plastid cytochrome *c* maturation seems in our sense the most compelling hypothesis, and we propose that it corresponds to an eighth assembly factor in the system II plastid pathway.

Emergence of a Thioreduction Pathway in Plastid c-Type Cytochrome Biogenesis—The existence of a thio-reduction pathway in the chloroplast was also suggested recently with the discovery of HCF164, a thylakoid membrane-anchored thioredoxin-like protein with disulfide reductase activity which is required for cytochrome b_6f biogenesis in *Arabidopsis* (62). HCF164 displays similarity to CcsX/ResA, a thioredoxin-like protein involved in system II bacterial cytochrome *c* assembly pathway (63, 64). Remarkably, CcsX, ResA, and HCF164 proteins share the same membrane topology with the thioredoxin-like domain facing the *p*-side of the membrane, suggesting that their relevant targets of action are also located in this compartment (62–64). The definitive placement of HCF164 in plastid cytochrome *c* maturation is still uncertain because the defect in cytochrome b_6f assembly could not be localized specifically to a block in the maturation of a particular subunit (*i.e.* conversion of apocytochrome *f* to its holoform) (62). A nucleus-encoded HCF164-like protein is also present in *Chlamydomonas*, but functional assignment in chloroplast cytochrome *c* biogenesis could not be provided in the algal system because none of the *ccs2* to *ccs6* mutations appears to lie in the HCF164-encoding gene.[8]

Erldensson and co-workers (28, 64) have proposed that ResA and CcdA are part of a redox relay required for the reduction of the cysteinyls in the heme binding site of apocytochrome *c*. Interestingly, we have noted that in cyanobacteria *Gloeobacter violaceus* and *Geobacter sulfurreducens*, CCDA and HCF164 homologs are encoded by adjacent genes (65, 66), giving support to the hypothesis that they might act together in a same redox pathway in the plastid. Immunoblotting experiments showed that HCF164 accumulation is not affected by loss-of-function alleles in *CCDA* (Fig. 7). This result, however, does not necessarily rule out a model in which CCDA and HCF164 are interacting partners involved in the same pathway, and we hypothesize that HCF164 is the ninth component involved in plastid cytochrome *c* formation. We propose that the transfer of electrons from the stroma to the lumen for maintenance of reduced C*XX*CH motif in apocytochrome *c* proceeds via sulfide/disulfide transporter CCDA and HCF164 thioredoxin (Fig. 8). We postulate that the provision of reducing equivalents in the plastid system is dependent upon other redox components, like for instance, a membrane-anchored thioredoxin-like protein on the *n*-side (Fig. 8). These redox components might correspond to the gene products of *CCS4* and *CCS5* loci in *Chlamydomonas* (17, 20). Indeed, a preliminary functional assessment of these genes in redox chemistry is based on the observation that *ccs4* and *ccs5* mutants, similar to *ccda* and *resA*/*ccsx* mutants in bacteria (26, 28, 63, 64), can be rescued for cytochrome *c* deficiency by exogenous reduced thiol compounds.[9] It is conceivable that, because of the compartmentalization of the thylakoid lumen, the redox pathway evolved in plastids relies on several players (at least CCDA, HCF164, Ccs4, and Ccs5) and is therefore more complex than its bacterial counterpart.

Acknowledgments—We thank L. Dolfini for technical assistance; Dr. U. Boronowsky for the generation of CCDA antisera, the sequencing 118B12T7 and F2D5T7 clones, and initial PhoA fusion constructs; and Dr. S. Nakamoto for sequencing LC074f09_r. We are grateful to Drs. A. Barkan (maize α-Rieske FeS), D. Krogmann (spinach α-cyt *f*), K. Meierhoff (*Arabidopsis* α-HCF164), J. L. Popot (*Chlamydomonas*

[7] We determined the genomic organization of the *CCDA* locus by sequencing.

[8] S. T. Gabilly, P. P. Hamel, and S. Merchant, unpublished data.

[9] P. P. Hamel and S. Merchant, unpublished data.

α-Cox1), N. Raikhel (*Arabidopsis* α-Sec12), and F.-A. Wollman (*Chlamydomonas* α-cyt b_6 and α-subunit IV/PetD) for the kind donation of antibodies. We also thank Dr. J. Gober for the gift of plasmid placZ290, Drs. J. Beckwith for the gift of plasmid pBAD22 and M. Ehrmann for the gift of strain LMG194.

REFERENCES

1. Thöny-Meyer, L. (1997) *Microbiol. Mol. Biol. Rev.* **61,** 337–376
2. Barker, P. D., and Ferguson, S. J. (1999) *Struct. Fold. Des.* **7,** 281–290
3. Allen, J. W., Daltrop, O., Stevens, J. M., and Ferguson, S. J. (2003) *Philos. Trans. R. Soc. Lond. B Biol. Sci.* **358,** 255–266
4. Kranz, R., Lill, R., Goldman, B., Bonnard, G., and Merchant, S. (1998) *Mol. Microbiol.* **29,** 383–396
5. Xie, Z., and Merchant, S. (1998) *Biochim. Biophys. Acta* **1365,** 309–318
6. Nakamoto, S. S., Hamel, P., and Merchant, S. (2000) *Biochimie* (*Paris*) **82,** 603–614
7. Thöny-Meyer, L. (2002) *Biochem. Soc. Trans.* **30,** 633–638
8. Ferguson, S. J. (2001) *Biochem. Soc. Trans.* **29,** 629–640
9. Allen, J. W. A., Barker, P. D., and Ferguson, S. J. (2003) *J. Biol. Chem.* **278,** 52075–52083
10. Kranz, R. G., Beckett, C. S., and Goldman, B. S. (2002) *Res. Microbiol.* **153,** 1–6
11. O'Brian, M. R., and Thöny-Meyer, L. (2002) *Adv. Microb. Physiol.* **46,** 257–318
12. Ortenberg, R., and Beckwith, J. (2003) *Antioxid. Redox Signal* **5,** 403–411
13. Kadokura, H., Katzen, F., and Beckwith, J. (2003) *Annu. Rev. Biochem.* **72,** 111–135
14. Fabianek, R. A., Hennecke, H., and Thöny-Meyer, L. (2000) *FEMS Microbiol. Rev.* **24,** 303–316
15. Ritz, D., and Beckwith, J. (2001) *Annu. Rev. Microbiol.* **55,** 21–48
16. Xie, Z., and Merchant, S. (1996) *J. Biol. Chem.* **271,** 4632–4639
17. Xie, Z., Culler, D., Dreyfuss, B. W., Kuras, R., Wollman, F. A., Girard-Bascou, J., and Merchant, S. (1998) *Genetics* **148,** 681–692
18. Inoue, K., Dreyfuss, B. W., Kindle, K. L., Stern, D. B., Merchant, S., and Sodeinde, O. A. (1997) *J. Biol. Chem.* **272,** 31747–31754
19. Dreyfuss, B. W., Hamel, P. P., Nakamoto, S. S., and Merchant, S. (2003) *J. Biol. Chem.* **278,** 2604–2613
20. Dreyfuss, B. W., and Merchant, S. (1999) in *Proceedings of the XIth International Congress on Photosynthesis* (Pusztai, J., and Garab, G., eds) Vol. IV, pp. 3139–3142, Kluwer Academic Publishers, The Netherlands
21. Hamel, P. P., Dreyfuss, B. W., Xie, Z., Gabilly, S. T., and Merchant, S. (2003) *J. Biol. Chem.* **278,** 2593–2603
22. Kimball, R. A., Martin, L., and Saier, M. H., Jr. (2003) *J. Mol. Microbiol. Biotechnol.* **5,** 133–149
23. Le Brun, N. E., Bengtsson, J., and Hederstedt, L. (2000) *Mol. Microbiol.* **36,** 638–650
24. Schiött, T., Throne-Holst, M., and Hederstedt, L. (1997) *J. Bacteriol.* **179,** 4523–4529
25. Schiött, T., von Wachenfeldt, C., and Hederstedt, L. (1997) *J. Bacteriol.* **179,** 1962–1973
26. Deshmukh, M., Brasseur, G., and Daldal, F. (2000) *Mol. Microbiol.* **35,** 123–138
27. Bardischewsky, F., and Friedrich, C. G. (2001) *J. Bacteriol.* **183,** 257–263
28. Erlendsson, L. S., and Hederstedt, L. (2002) *J. Bacteriol.* **184,** 1423–1429
29. Hofmann, N. R., and Theg, S. M. (2003) *Plant Mol. Biol.* **53,** 643–654
30. Monika, E. M., Goldman, B. S., Beckman, D. L., and Kranz, R. G. (1997) *J. Mol. Biol.* **271,** 679–692
31. Ehrmann, M., Boyd, D., and Beckwith, J. (1990) *Proc. Natl. Acad. Sci. U. S. A.* **87,** 7574–7578
32. Guzman, L. M., Belin, D., Carson, M. J., and Beckwith, J. (1995) *J. Bacteriol.* **177,** 4121–4130
33. Brickman, E., and Beckwith, J. (1975) *J. Mol. Biol.* **96,** 307–316
34. Kranz, R. G., and Haselkorn, R. (1985) *Gene* (*Amst.*) **40,** 203–215
35. Pollock, M. A., and Oppenheimer, D. G. (1999) *BioTechniques* **26,** 254–257
36. Lukowitz, W., Gillmor, C. S., and Scheible, W.-R. (2000) *Plant Physiol.* **123,** 795–806
37. Klimyuk, V. I., Carroll, B. J., Thomas, C. M., and Jones, J. D. (1993) *Plant J.* **3,** 493–494
38. Smith, P. K., Krohn, R. I., Hermanson, G. T., Mallia, A. K., Gartner, F. H., Provenzano, M. D., Fujimoto, E. K., Goeke, N. M., Olson, B. J., and Klenk, D. C. (1985) *Anal. Biochem.* **150,** 76–85
39. Quinn, J. M., and Merchant, S. (1998) *Methods Enzymol.* **297,** 263–279
40. Page, M. D., and Ferguson, S. J. (1989) *Mol. Microbiol.* **3,** 653–661
41. Sarsero, J., and Pittard, A. (1995) *J. Bacteriol.* **177,** 297–306
42. Sussman, M. R., Amasino, R. M., Young, J. C., Krysan, P. J., and Austin-Phillips, S. (2000) *Plant Physiol.* **124,** 1465–1467
43. Alonso, J. M., Stepanova, A. N., Leisse, T. J., Kim, C. J., Chen, H., Shinn, P., Stevenson, D. K., Zimmerman, J., Barajas, P., Cheuk, R., Gadrinab, C., Heller, C., Jeske, A., Koesema, E., Meyers, C. C., Parker, H., Prednis, L., Ansari, Y., Choy, N., Deen, H., Geralt, M., Hazari, N., Hom, E., Karnes, M., Mulholland, C., Ndubaku, R., Schmidt, I., Guzman, P., Aguilar-Henonin, L., Schmid, M., Weigel, D., Carter, D. E., Marchand, T., Risseeuw, E., Brogden, D., Zeko, A., Crosby, W. L., Berry, C. C., and Ecker, J. R. (2003) *Science* **301,** 653–657
44. Martienssen, R. A. (1998) *Proc. Natl. Acad. Sci. U. S. A.* **95,** 2021–2026
45. Grevelding, C., Fantes, V., Kemper, E., Schell, J., and Masterson, R. (1993) *Plant Mol. Biol.* **23,** 847–860
46. Meurer, J., Meierhoff, K., and Westhoff, P. (1996) *Planta* **198,** 385–396
47. Bruce, B. D. (2001) *Biochim. Biophys. Acta* **1541,** 2–21
48. Lorkovic, Z., Schroder, W., Pakrasi, H., Irrgang, K., Herrmann, R., and Oelmuller, R. (1995) *Proc. Natl. Acad. Sci. U. S. A.* **92,** 8930–8934
49. Tissier, C., Woolhead, C. A., and Robinson, C. (2002) *Eur. J. Biochem.* **269,** 3131–3141
50. Katzen, F., and Beckwith, J. (2003) *Proc. Natl. Acad. Sci. U. S. A.* **100,** 10471–10476
51. Cocherel, S., Perez, P., Degroote, F., Genestier, S., and Picard, G. (1996) *Plant Mol. Biol.* **30,** 539–551
52. Dubreucq, B., Berger, N., Vincent, E., Boisson, M., Pelletier, G., Caboche, M., and Lepiniec, L. (2000) *Plant J.* **23,** 643–652
53. Kuras, R., and Wollman, F. A. (1994) *EMBO J.* **13,** 1019–1027
54. Weigel, M., Pesaresi, P., and Leister, D. (2003) *Trends Plant Sci.* **8,** 513–517
55. Gupta, R., He, Z., and Luan, S. (2002) *Nature* **417,** 567–571
56. Howe, G., and Merchant, S. (1992) *EMBO J.* **11,** 2789–2801
57. Howe, G., and Merchant, S. (1993) *Proc. Natl. Acad. Sci. U. S. A.* **90,** 1862–1866
58. Howe, G., and Merchant, S. (1994) *J. Biol. Chem.* **269,** 5824–5832
59. Howe, G., Mets, L., and Merchant, S. (1995) *Mol. Gen. Genet.* **246,** 156–165
60. Kurisu, G., Zhang, H., Smith, J. L., and Cramer, W. A. (2003) *Science* **302,** 1009–1014
61. Stroebel, D., Choquet, Y., Popot, J. L., and Picot, D. (2003) *Nature* **426,** 413–418
62. Lennartz, K., Plücken, H., Seidler, A., Westhoff, P., Bechtold, N., and Meierhoff, K. (2001) *Plant Cell* **13,** 2539–2551
63. Beckett, C. S., Loughman, J. A., Karberg, K. A., Donato, G. M., Goldman, W. E., and Kranz, R. G. (2000) *Mol. Microbiol.* **38,** 465–481
64. Erlendsson, L. S., Acheson, R. M., Hederstedt, L., and Le Brun, N. E. (2003) *J. Biol. Chem.* **278,** 17852–17858
65. Methé, B. A., Nelson, K. E., Eisen, J. A., Paulsen, I. T., Nelson,W., Heidelberg, J. F., Wu, D., Wu, M., Ward, N., Beanan, M. J., Dodson, R. J., Madupu, R., Brinkac, L. M., Daugherty, S. C., DeBoy, R. T., Durkin, A. S., Gwinn, M., Kolonay, J. F., Sullivan, S. A., Haft, D. H., Selengut, J., Davidsen, T. M., Zafar, N., White, O., Tran, B., Romero, C., Forberger, H. A., Weidman, J., Khouri, H., Feldblyum, T. V., Utterback, T. R., Van Aken, S. E., Lovley, D. R., and Fraser, C. M. (2003) *Science* **302,** 1967–1969
66. Nakamura, Y., Kaneko, T., Sato, S., Mimuro, M., Miyashita, H., Tsuchiya, T., Sasamoto, S., Watanabe, A., Kawashima, K., Kishida, Y., Kiyokawa, C., Kohara, M., Matsumoto, M., Matsuno, A., Nakazaki, N., Shimpo, S., Takeuchi, C., Yamada, M., and Tabata, S. (2003) *DNA Res.* **10,** 137–145
67. Rost, B., Fariselli, P., and Casadio, R. (1996) *Protein Sci.* **5,** 1704–1718
68. Seki, M., Narusaka, M., Kamiya, A., Ishida, J., Satou, M., Sakurai, T., Nakajima, M., Enju, A., Akiyama, K., Oono, Y., Muramatsu, M., Hayashizaki, Y., Kawai, J., Carninci, P., Itoh, M., Ishii, Y., Arakawa, T., Shibata, K., Shinagawa, A., and Shinozaki, K. (2002) *Science* **296,** 141–145
69. Tabata, S., Kaneko, T., Nakamura, Y., Kotani, H., Kato, T., Asamizu, E., Miyajima, N., Sasamoto, S., Kimura, T., Hosouchi, T., Kawashima, K., Kohara, M., Matsumoto, M., Matsuno, A., Muraki, A., Nakayama, S., Nakazaki, N., Naruo, K., Okumura, S., Shinpo, S., Takeuchi, C., Wada, T., Watanabe, A., Yamada, M., Yasuda, M., Sato, S., de la Bastide, M., Huang, E., Spiegel, L., Gnoj, L., O'Shaughnessy, A., Preston, R., Habermann, K., Murray, J., Johnson, D., Rohlfing, T., Nelson, J., Stoneking, T., Pepin, K., Spieth, J., Sekhon, M., Armstrong, J., Becker, M., Belter, E., Cordum, H., Cordes, M., Courtney, L., Courtney, W., Dante, M., Du, H., Edwards, J., Fryman, J., Haakensen, B., Lamar, E., Latreille, P., Leonard, S., Meyer, R., Mulvaney, E., Ozersky, P., Riley, A., Strowmatt, C., Wagner-McPherson, C., Wollam, A., Yoakum, M., Bell, M., Dedhia, N., Parnell, L., Shah, R., Rodriguez, M., See, L. H., Vil, D., Baker, J., Kirchoff, K., Toth, K., King, L., Bahret, A., Miller, B., Marra, M., Martienssen, R., McCombie, W. R., Wilson, R. K., Murphy, G., Bancroft, I., Volckaert, G., Wambutt, R., Dusterhoft, A., Stiekema, W., Pohl, T., Entian, K. D., Terryn, N., Hartley, N., Bent, E., Johnson, S., Langham, S. A., McCullagh, B., Robben, J., Grymonprez, B., Zimmermann, W., Ramsperger, U., Wedler, H., Balke, K., Wedler, E., Peters, S., van Staveren, M., Dirkse, W., Mooijman, P., Lankhorst, R. K., Weitzenegger, T., Bothe, G., Rose, M., Hauf, J., Berneiser, S., Hempel, S., Feldpausch, M., Lamberth, S., Villarroel, R., Gielen, J., Ardiles, W., Bents, O., Lemcke, K., Kolesov, G., Mayer, K., Rudd, S., Schoof, H., Schueller, C., Zaccaria, P., Mewes, H. W., Bevan, M., Fransz, P., Kazusa DNA Research Institute, Cold Spring Harbor and Washington University in St. Louis Sequencing Consortium, and European Union *Arabidopsis* Genome Sequencing Consortium (2000) *Nature* **408,** 823–826
70. Nunberg, J. H., Kaufman, R. J., Chang, A. C., Cohen, S. N., and Schimke, R. T. (1980) *Cell* **19,** 355–364
71. Wingrove, J. A., Mangan, E. K., and Gober, J. W. (1993) *Genes Dev.* **7,** 1979–1992

Figure Legends for supplemental data:

Figure 1: Alignment of bacterial and eukaryotic CcdA homologs

CcdA homologs from genomes of vascular plants *Arabidopsis thaliana* (AAF35369), *Descurainia sophia* (AAQ95739), *Glycine max* (AAP81162), *Hordeum vulgare* (AAO16019), *Lotus japonicus* (AAO16018) and *Medicago truncatula* (AAO16020), green alga *Chlamydomonas reinhardtii* (AAL84598), red alga *Porphyra purpurea* (U38804), and bacteria *Rhodobacter capsulatus* (AAF26218), *Paracoccus pantotrophus* (AAG29835) and *Bacillus subtilis* (P45706) were aligned using the CLUSTALW algorithm (Blosum62 scoring matrix) in Bioedit software. Aligned sequences were edited manually in the GeneDoc multiple alignment editor software. Amino-acids strictly conserved in all sequences are shaded blue and those conserved in 8 of 11 sequences are shaded red. The two conserved redox active cysteine residues are highlighted in yellow. The protein sequence corresponding to the six predicted transmembrane domains (1 to 6) is underlined by a thick line. The putative recognition site (AXA↓) for cleavage by the thylakoid processing peptidase (TPP) is indicated in purple.

Figure 2: Southern blot analysis of *ccda-1* and *ccda-4* mutant lines

Panel A: Southern blot analysis of progeny arising from self-pollination of heterozygous ccda-1 lines. Genomic DNA was digested with *Cla*I and separated through agarose gel electrophoresis. Following electrophoresis, DNA was transferred to a nylon membrane and hybridized with a radio-labelled probe comprising the *nptII* gene. The membrane was scanned by phosphorimaging after 72h of exposition. Molecular weights (kb) of hybridizing bands are shown on the right side. Lanes: 1, line carrying no T-DNA (wild type segregant), 2, line carrying only the additional T-DNA, 3, line carrying the *ccda::T-DNA* (*ccda-1*) allele and 4, line carrying *ccda::T-DNA* (*ccda-1* allele) and additional T-DNA.

Panel B: Southern blot analysis indicating the presence of one T-DNA per genome in the ccda-4 mutant line. Genomic DNA from heterozygous *ccda-4* plants was digested with *Hind*III and separated through agarose gel electrophoresis. Following electrophoresis, DNA was transferred to a nylon membrane and hybridized with a radio-labelled probe containing the *CaMV35S* promoter. The membrane was scanned using phosphorimager after 96h of exposure. Molecular weights (kb) of hybridizing bands are shown at right. Lanes: 1, wild type (Col-0), 2, *CCDA*/*ccda::T-DNA* (*ccda-1*) hemizygous plant.

Figure 3: PCR analysis of T-DNA/Ds insertions structures in the *ccda* mutant lines

PCR amplification was performed as described in experimental procedures using plant genomic DNA as a template and diagnostic primers (see table I supplemental data). The products were analyzed by agarose electrophoresis and stained using ethidium bromide. Pictures of the stained gels are shown in the figure. For the *ccda-1* line, T-DNA specific primers were JL-202 (left border) and XR-2 (right border) and *CCDA*-specific primers were CCDA-F7, CCDA-F8, CCDA-R7 and CCDA-R8. For the *ccda-2* line, Ds element-specific primers were Ds5.1 (5') and Ds3.1 (3') and *CCDA*-specific primers were CCDA-F3, CCDA-F4, CCDA-R9 and CCDA-R12. For the *ccda-3* line, T-DNA specific primers were ROK2-LB1 (left border) and ROK2-RB1 (right border) and *CCDA*-specific primers were CCDA-F3, CCDA-F9, CCDA-R9 and CCDA-R12. For *the ccda-4* line, T-DNA specific primers were ROK2-LB1 (left border) and ROK2-RB1 (right border) and *CCDA*-specific primers were CCDA-F11, CCDA-F12, CCDA-R14 and CCDA-R15.

Table supplemental material

Table I

Oligonucleotides primers used for PCR amplification

Primers used for in vitro import constructs	
DHFR-F1	TTG**aggcct**CATGGTTCGACCATTGAA
DHFR-R1	CCC**tctaga**TTAGTCTTTCTTCTCGTAGA
PCGEN-F1	AATGCCACGTCACCTCACAAACATCTAG
PCGEN-R1	CTCGTCTTCGTCGAACACCACGTTATGTG
PCSS-F3	CCCG**gaattc**GATCAACAAAACACCCCAAAAA
PCSS-R2	CCA**aggcct**TCAGATGGTACGAAAGCAA
Primers used for construction of CCDA-PhoA and –LacZ fusions	
NT	TTCC**ggtacc**CATGAATCTGAGTGTGAAC
CT-I	TTCC**tctaga**CCGACCGAATCTCCAAGGCT
CT-II	TTCC**tctaga**CCAGACCCAAATGCACCAAT
CT-III	TTCC**tctaga**CCATAGGCTTTTCCGGC
CT-IV	TTCC**tctaga**TTAAAGAAAGAAGGAAGCTG
CT-V	TTCC**tctaga**CCAAGAAGAGTGGCTAGAAC
CT-VI	TTCC**tctaga**ACCTTTCGCAACGAAAGTAAGCTCTG
CT-VII	TTCC**tctaga**ACCATAGTAGCAGCAGGAAAAAG
LacZ-F1	TTCC**tctaga**CGTCGTTTTACAACGTC
LacZ-R1	TTCCTT**gcatgc**GGTTATTATTATTTTTGAC
SW-KpnI	CGG**ggtacc**TAATCTGAGTGTGAAC
SW2-1	CGG**ggtacc**CCATAGGCTTTTCCGC
SW2-2	TCCAAATAGGACAAGGATTACCAG
SW-Stop	ATTACATGACCATAGTAGCAGCAGG
SW-KpnIbis	TTCC**ggtacc**TAATCTGAGTGTGAAC
SW3-2	TCGCTGCAGCAGCAAACTTCCCATC
SW3-3	TTCC**ggtacc**CGAGGATCAAGTTGTTAAAG
***CCDA* specific primers**	
CCDA-F3	TGGGCTTGTAAACATAAGCTTAGTACCAT
CCDA-F4	GGATCCATAGTGACTTTGTACACTCCAAT
CCDA-F6	ATAGGCTTTTTCCTGCTGCTACTATGGTC
CCDA-F7	CATTCTGTTATTGTTCTGTGGCATG
CCDA-F8	AGGTAATGTTGTCACTACTCTCTTCTCAC
CCDA-F9	CACACTACTCATTAGCCCACTCAACATTA
CCDA-F11	TAGCTGCAGACTCAATCATGGTAGTGATG
CCDA-F12	TCGTTCGCATAGCGCTTGGAATTACTGTG
CCDA-R5	AATACAATGAAATGGTAAATGGAGGGACT
CCDA-R7	ATGGTCAAGGTCTCAGAAACGCGTTCATTG
CCDA-R8	GCCAAACTACAACAGGGATAAATTAGCAG
CCDA-R9	GTGAGAAGAGAGTAGTGACAACATTACCT
CCDA-R12	CACAGTAATTCCAAGCGCTATGCGAAGCA
CCDA-R14	CCTTACCAAGACAATCATCTTCAAGTCTG
CCDA-R15	CTTTTGCTGAGCTAAGAGTTACCAAGTTC

Table I

Oligonucleotides primers used for PCR amplification

T-DNA / Ds – specific primers	
JL-202	CATTTTATAATAACGCTGCGGACATCTAC
JL-270	TTTCTCCATATTGACCATCATACTCATTG
XR-2	TGGGAAAACCTGGCGTTACCCAACTTAAT
XR-3	TGGCGAATGAGACCTCAATTGCGAGCTTT
Ds3.1	TTCGTTACCGGTATATCCCGTTTTCGTTT
Ds3.2	TTTTACCGACCGTTACCGACCGTTTTCAT
Ds5.1	CTCGGGTTCGAAATCGATCGGGATAAAAC
Ds5.2	CAAAATCGGTTATACGATAACGGTCGGTA
ROK2-LB1	GTTGCCCGTCTCACTGGTGAAAAGAAAAA
ROK2-LB2	CAGTACATTAAAAACGTCCGCAATGTGT
ROK2-RB1	CGTATGTGCTTAGCTCATTAAACTCCAGA
ROK2-RB2	TGCGGTTCTGTCAGTTCCAAACGTAAAAC
Primers used for amplification of DNA probes (Southern blots)	
NPT2-F2	ATCTCACCTTGCTCCTGCCGAGAAAGTAT
NPT2-R2	AGAAGAACTCGTCAAGAAGGCGATAGAAG
35S-F2	CAAATACCTTCCCAAGAAGGTTAAAGATG
35S-R1	TGTCCTCTCCAAATGAAATGAACTTCCTT
35S-R2	GCATCTTGAACGATAGCCTTTCCTTTATC
Primers used for RT-PCR experiments	
PetA-L	TTTCTTGGATAAGGGAAGAG
PetA-R	GCAATTGGCACATACAATAC
PetB-L	TAACTTGGGTTACTGGTGTG
PetB-R	TTGTCCAACACTAGCACTTC
LB-RT1	CATTAAAAACGTCCGCAATGT
Ds-RT1	CGTTACCGACCGTTTTCATC
RT-R4	CCCATTACAATAGCCAGACC
RT-F5	TAGTGTTTTGCCGTTGACAC
RT-F12	CATGAATCTGAGTGTGAACC

Primers were obtained from Sigma Genosys, The Woodlands, TX, and from Integrated DNA Technologies, Coralville, IA. The bold lower case letters indicate the nucleotide change in the PCR primers resulting in the introduction of a restriction site in the amplified DNA.

Supplemental material for experimental procedures

Plasmids and DNAs used in this study: The Arabidopsis *CCDA* cDNA clones 118B12T7 and F2D5T7 were obtained from the MSU-DOE Plant research Laboratory, Michigan State University, Lansing, MI. The Arabidopsis *CCDA* cDNA in clone 118B12T7 contained a 1062 bp open reading frame, the ATG start codon of which was the most 5' ATG codon. The subsequently published sequence of the RIKEN full-length cDNA clone RAFL08-16-A19 (68) indicated the presence of an in-frame stop codon 30 bp upstream of this ATG codon, confirming it as the start codon for the ORF. The sequenced cDNAs (AAF35369) derive from the *A. thaliana* nuclear gene At5g54290 (NC_003076) (69). Clones LC074f09_r and MWM005e08_r were purchased from the Kasuza DNA Research Institute, Tokyo, Japan. Clone Hv_CEb0011A16f was provided by the Clemson University Genomics Institute, Clemson, SC and clone NF018C09LF was from the Samuel Roberts Noble Foundation, Ardmore, OK. Clones Ds01-15L12 and Gm01_13a12 were obtained from the Eastern Cereal and Oilseed Research Centre, Ottawa, Canada, respectively. Plasmid pLITMUS28 and pGEM2 were obtained from Promega Corp., Madison, WI. Plasmid pD991 was the kind gift of Prof. T. Jack, Dartmouth College, NH. Plasmid pFT-1, containing mDHFR cDNA (70), was kindly provided by Prof. C. Koehler, UCLA, CA.

Constructs for chloroplast import experiments: To construct plasmid pGEM2-AtCCDA, the *A. thaliana CCDA* cDNA was subcloned as an *Eco*RI / *Xba*I fragment into pGEM2 from pZL118 carrying the 118B12T7 cDNA. Construction of the CCDA-DHFR fusion was facilitated by the presence of a *Stu*I site in the DNA region predicted to encode the N-terminal portion of the first transmembrane helix of the CCDA polypeptide. The entire mouse DHFR coding region (mDHFR) was PCR amplified from pFT-1 as a template with primers DHFR-F1 and DHFR-R1, which added *Stu*I and *Xba*I restriction sites in the 5'and 3' regions of the DHFR cDNA. Plasmid pFT-1 was denatured for 5 minutes at 94 °C and a two-stage amplification was

performed (15 sec at 94 °C, 30 sec at 45 °C and 60 sec at 72 °C, 5 cycles; then 15 sec at 94 °C, 30 sec at 55 °C and 60 sec at 72 °C, 20 cycles). The 583 bp PCR product was isolated and cloned in *Eco*RV-digested pLITMUS28. Sequencing of the insert confirmed that no mutations had been introduced. The DHFR gene sequence was then excised with *Stu*I and *Xba*I and cloned in *Stu*I/*Xba*I digested pZL118. The resulting plasmid carries the 141 amino-terminal of CCDA in frame with DHFR. The CCDA-DHFR construct was then sub-cloned as an *Eco*RI-*Xba*I fragment in pGEM2. The resulting plasmid, termed pGEM2-AtCCDA-DHFR, was sequenced to confirm production of an in-frame gene fusion.

A DNA fragment encompassing the *A. thaliana PETE1* (plastocyanin) transit peptide encoding region (502 bp) was amplified from Col-0 genomic DNA using primers PCGEN-F1 and PCGEN-R1, cloned in *Eco*RV digested pLITMUS28, and sequenced. The cloned DNA was then used as a template for a second round of PCR amplification using primers PCSS-F3 and PCSS-R2, which were designed to amplify the *PETE1* transit peptide encoding sequence engineered with *Eco*RI (5') and *Stu*I (3') restriction sites. The template was denatured for 5 minutes at 94 ºC and a two-stage amplification performed (15 sec at 94 °C, 30 sec at 45 °C, 45 sec at 72 °C, 2 cycles; then 15 sec at 94 °C, 30 sec at 55 °C, 45 sec at 72 °C, 18 cycles). The 319 bp PCR product was cloned in *Eco*RV digested pLITMUS28, and sequenced. The *PETE1* transit sequence was then excised with *Eco*RI plus *Stu*I and subcloned in *Eco*RI/*Stu*I digested pGEM2-AtCCDA-DHFR. The resulting plasmid, termed pGEM2-AtPETE1–DHFR was verified by sequencing and carries as expected a fusion encoding the 77 amino-acid of plastocyanin transit sequence plus the first 5 residues of the mature protein in frame with DHFR.

Construction of CCDA-phoA, CCDA-lacZ and CCDA-phoA sandwich fusions: Various portions of the *CCDA* ORF were amplified with *Pfu* polymerase using the cloned *CCDA* cDNA (AF225913) as a template, NT1 as a forward primer and one of the 7 CT oligonucleotides as a reverse primer (see table I supplemental material). NT1 primer was

engineered with a *Kpn*I site upstream of the first ATG codon in *CCDA* cDNA (6) and reverse primers were designed with an *Xba*I site at the desired *CCDA-phoA* fusion junction. PCR products thus obtained were digested with *Kpn*I and *Xba*I and cloned into *Kpn*I/*Xba*I digested pRGK200 -containing the alkaline phosphatase encoding gene (*phoA*)- to generate the p*CCDA::phoA* series of plasmids. The *CCDA-phoA* translational fusions (I to VII) were devised at positions 107, 181, 202, 236, 277, 322 and 353, respectively, of CCDA polypeptide. All the *CCDA–lacZ* fusions were constructed by replacing the 1.3 Kb *Xba*I/*Sph*I fragment carrying the *phoA* piece, in each p*CCDA::phoA* plasmid, with the full length *lacZ* gene in frame with the upstream *CCDA* coding sequence. LacZ F1 forward primer and LacZ R1 reverse primer containing respectively, an *Xba*I site and an *Sph*I site, were used to amplify the 3 kb *lacZ* gene from the placZ290 plasmid (71) as a template with TAKARA LA polymerase (TAKARA Bio Inc., Shiga, Japan). Each p*CCDA::phoA* plasmid was digested by *Xba*I and *Sph*I, isolated and ligated to *Xba*I/*Sph*I digested *LacZ* PCR product in order to generate the pCCDA::LacZ serie of plasmids.

For each sandwich fusion, an intact *CCDA* gene carrying a *phoA* in-frame insertion was reconstituted by PCR amplification using a two step cloning strategy. First, the DNA sequence corresponding to the C-terminal part of CCDA protein in SW_A and SW_B sandwich fusions was amplified using the cloned *CCDA* cDNA as a template and SW2-2/SWstop or SW3-2/SWstop as primers, respectively. The PCR products were cloned in pBAD22 at the *Hind*III site (located at the 3' end of *phoA*) which was filled in with the Klenow fragment of DNA polymerase prior to ligation. Recombinant plasmids carrying the *CCDA* sequence in the sense orientation with respect to the *phoA* gene were identified by diagnostic PCR screening and the integrity of the *phoA-CCDA* junction site was further confirmed by DNA sequencing. Recombinant plasmids carrying the *phoA-CCDA* fused sequences at position 202 and 242 of CCDA were named pSW_A and pSW_B, respectively. The coding sequence corresponding to the N-terminal part of CCDA was generated by PCR using SWKpnI/SW2-1 primers for SW_A and SWKpnIbis/SW3-3 primers for SW_B. All four primers were designed with a *Kpn*I site in

order to facilitate cloning of the PCR fragment at the *Kpn*I site upstream of the *phoA* gene in pBAD22. The intact CCDA-PhoA sandwich fusion was reconstituted by cloning of *Kpn*I-digested PCR fragments at the *Kpn*I site of pSW_A and pSW_B. Recombinant molecules carrying the CCDA N-terminal part in phase with the PhoA moiety were identified by diagnostic PCR.

RT-PCR experiments: The reverse transcription reaction was performed in 20 μl volume using the RT system (Promega). Total RNA (1 μg) was used as template for the AMV Reverse transcriptase in the presence of 0.5 μg of oligo$(dT)_{15}$ primer according to the manufacturer's instructions. Following the first strand synthesis, the resulting cDNAs were diluted 10 times and 10 μl was used to carry out the PCR amplification. The following parameters were used: for amplification of *CCDA*-specific fragments: 95°C for 30 sec, 55°C for 1 min and 72°C for 40 sec, 29 cycles. For *petA* and *petB* specific PCR amplification, the same cycling was used except that the annealing temperature was 50°C.

Screening and molecular characterization of ccda mutant lines: X and H pools of genomic DNAs from the Arabidopsis Knockout Facility were screened using the T-DNA left border primer JL-202 and the *CCDA*-specific primers CCDA-F3 and CCDA-R5. PCR reactions were analyzed for the presence of products hybridizing to a probe comprising the whole *CCDA* gene. In the first round of screening, one X pool was identified which gave a PCR product of 2.5 kb with JL-202 and CCDA-R5 primers hybridizing with the *CCDA* probe. The same X pool also gave a hybridizing PCR product of 1.5 kb when JL-202 and CCDA-F3 primers were used, suggesting the presence of an inverted tandem T-DNA insertion (see results section). The JL-202-CCDA-R5 PCR product was re-amplified (5 min at 94 °C, 15 sec at 94 °C, 30 sec at 65 °C, 45 sec-2 min at 72 °C, 25 cycles) using the same primers and a T-DNA insertion in the *CCDA* gene was confirmed by sequencing. Genomic DNA prepared from germinated J pool seeds and individual plants from the positive J pool were screened using

JL-202 and the *CCDA*-specific primer CCDA-R7. The single plant identified was designated CSJ6266.39.

For plants descending from CSJ6266.39, primers JL-202 plus CCDA-R7 were used to detect the *ccda-1* allele and CCDA-F8 plus CCDA-R7 to detect the *CCDA* wild type allele. For plants descending from the ET5250 line, Ds3.1 plus CCDA-R9 were used to detect the *ccda-2* allele and CCDA-F4 plus CCDA-R9 to detect the *CCDA* wild type allele. For plants descending from the SALK_025766 line, ROK2-LB1 plus CCDA-F4 were used to detect the *ccda-3* allele and CCDA-F4 plus CCDA-R12 to detect the *CCDA* wild type allele. For plants descending from the SALK_014416 line, ROK2-LB1 plus CCDA-R15 were used to detect the *ccda-4* allele and CCDA-F12 plus CCDA-R9 to detect the *CCDA* wild type allele. Primers CCDA-F6 and CCDA-R5 were used to check for recovery of genomic DNA in conditions where the diagnostic primers are not expected to give an amplification product.

For sequencing of the T-DNA integration junctions in *ccda-1*, PCR products resulting from amplification with JL-202 plus CCDA-F7 and JL-202 plus CCDA-R7 were re-amplified using JL-270 plus CCDA-F7 and JL-270 plus CCDA-R7 respectively. In the case of *ccda-3*, products resulting from amplification with ROK2-LB1 plus CCDA-F3 and ROK2-LB1 plus CCDA-R12 were re-amplified using ROK2-LB1 plus CCDA-F9 and ROK2-LB1 plus CCDA-R9 respectively. For *ccda-4*, products resulting from amplification with ROK2-LB1 plus CCDA-F11 and ROK2-LB1 plus CCDA-R14 were reamplified using ROK2-LB2 plus CCDA-F12 and ROK2-LB2 plus CCDA-R15, respectively. For sequencing of the Ds element integration juctions in lines carrying the *ccda-2* allele, PCR products resulting from amplification with Ds5.1 plus CCDA-F3 and Ds3.1 plus CCDA-R9 were re-amplified using Ds5.1 plus CCDA-F4 and Ds3.2 plus CCDA-R12, respectively. Re-amplification programs comprised: 5 mins at 94 °C; 15 sec at 94 °C, 30 sec at 55 °C, 45-90 sec at 72 °C, 20-25 cycles. The resulting PCR products were gel purified and cloned in *EcoR*V-digested pLITMUS28 for sequencing.

For the AKF screening, a 3.5 kb probe, comprising the whole *CCDA* gene plus upstream and downstream DNA, was amplified from wild-type genomic DNA using primers CCDA-F3 and CCDA-R5. The product of this reaction was used as the template in a second round of amplification using the same primers (5 mins at 94 °C, 15 sec at 94 °C, 30 sec at 65 °C, 2 min at 72 °C, 12 cycles). For analysis of *ccda-1* lines, a probe comprising a 429 bp segment of the T-DNA *nptII* gene was amplified from pD991 using primers NPT2-F2 and NPT2-R2 (5 mins at 94 °C; 15 sec at 94 °C, 30 sec at 45 °C, 60 sec at 72 °C, 25 cycles). For molecular analysis of the *ccda-4* line, a probe comprising a 527 bp segment of the T-DNA CaMV promoter was amplified from *ccda-4* genomic DNA. A 723 bp region of the promoter was amplified using primers 35S-F2 and 35S-R1. The product of this reaction was used as the template in a second round of amplification using primers 35S-F2 and 35S-R2 (5 mins at 94 °C; 15 sec at 94 °C, 30 sec at 55 °C, 60 sec at 72 °C, 25 cycles), yielding a 527 bp product. The PCR products were cloned in *Eco*RV digested pLITMUS28 and sequenced to confirm their identities. To generate probes, inserts were excised with *Eco*RI plus *Hin*dIII, isolated, and labelled with [α-^{32}P]dCTP by random priming.

Figure 1 Supplemental data

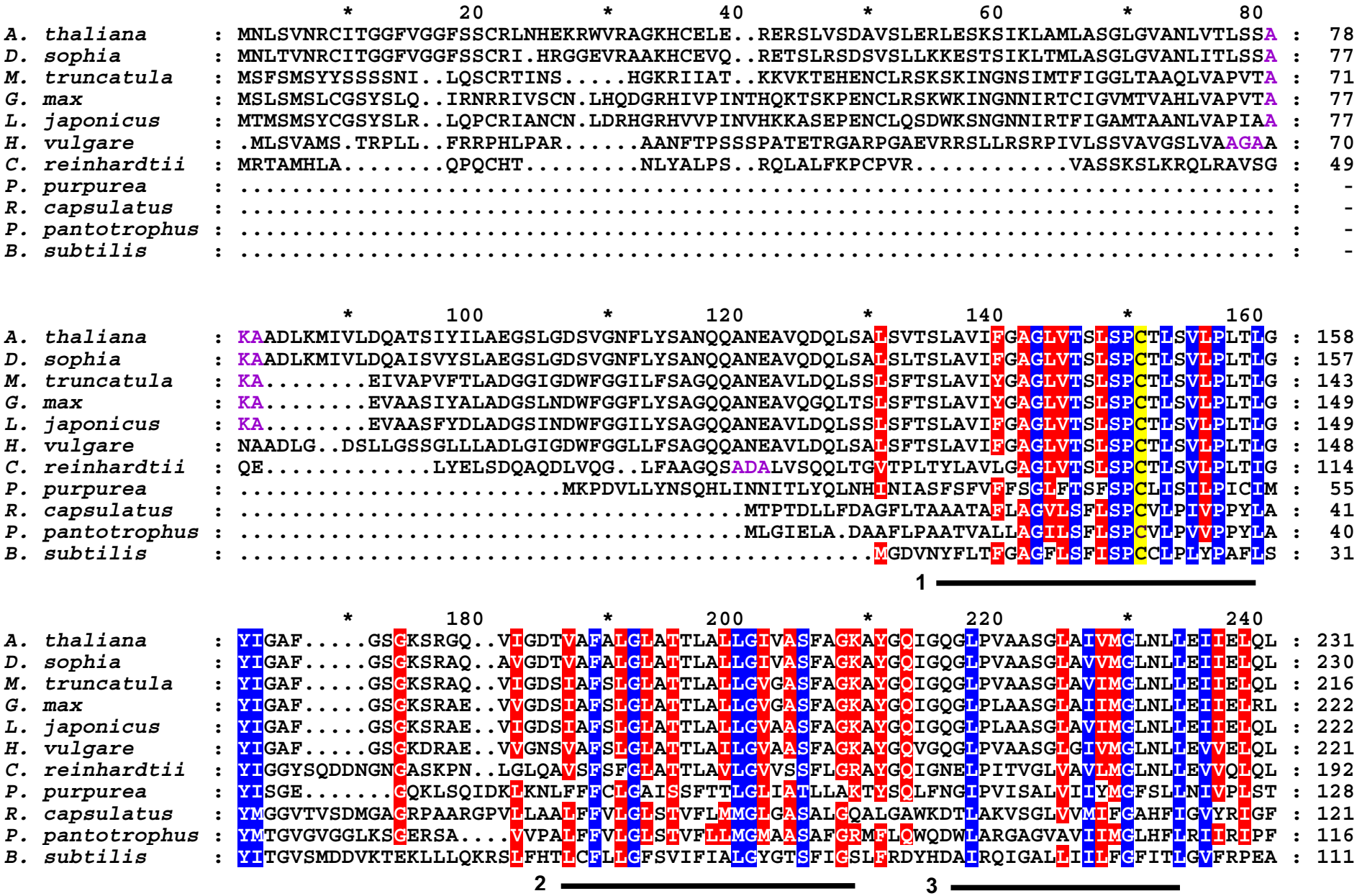

Figure 1 Supplemental data

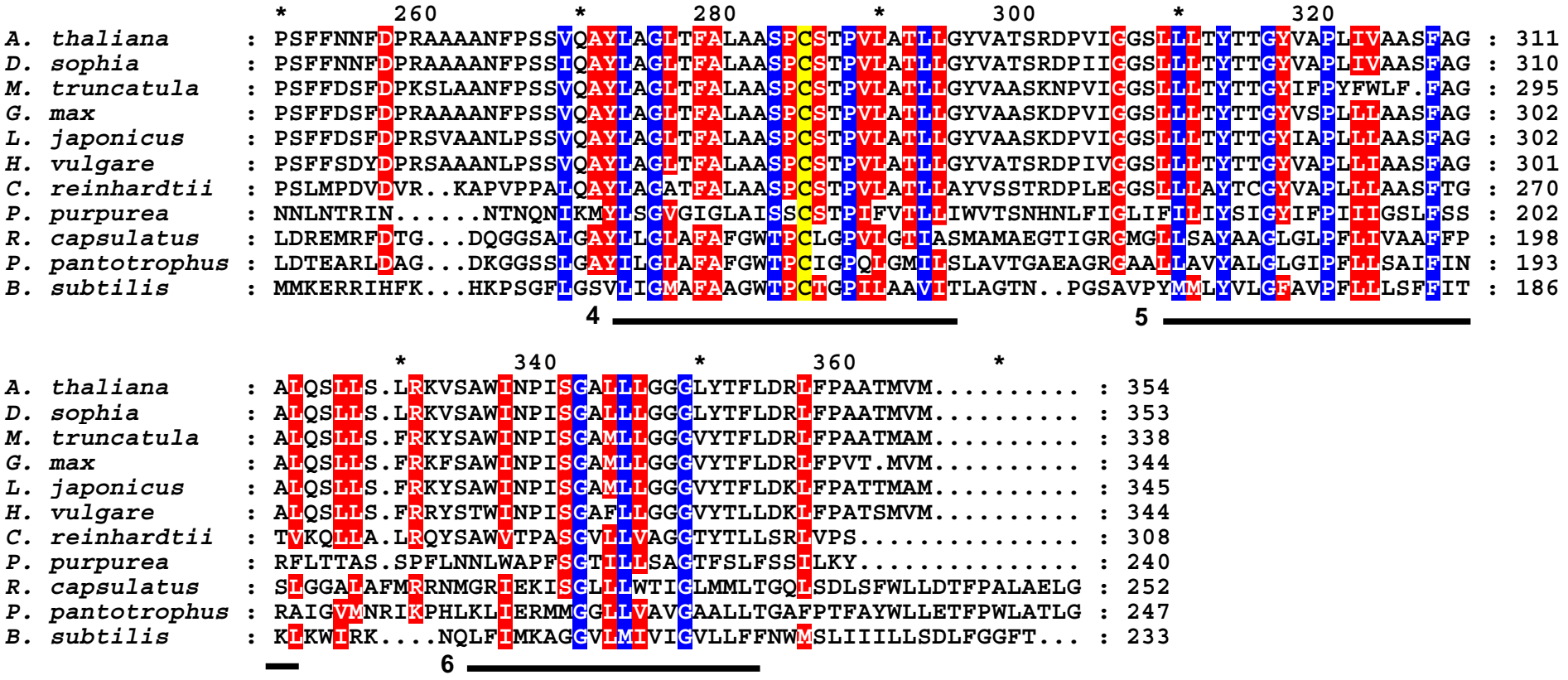

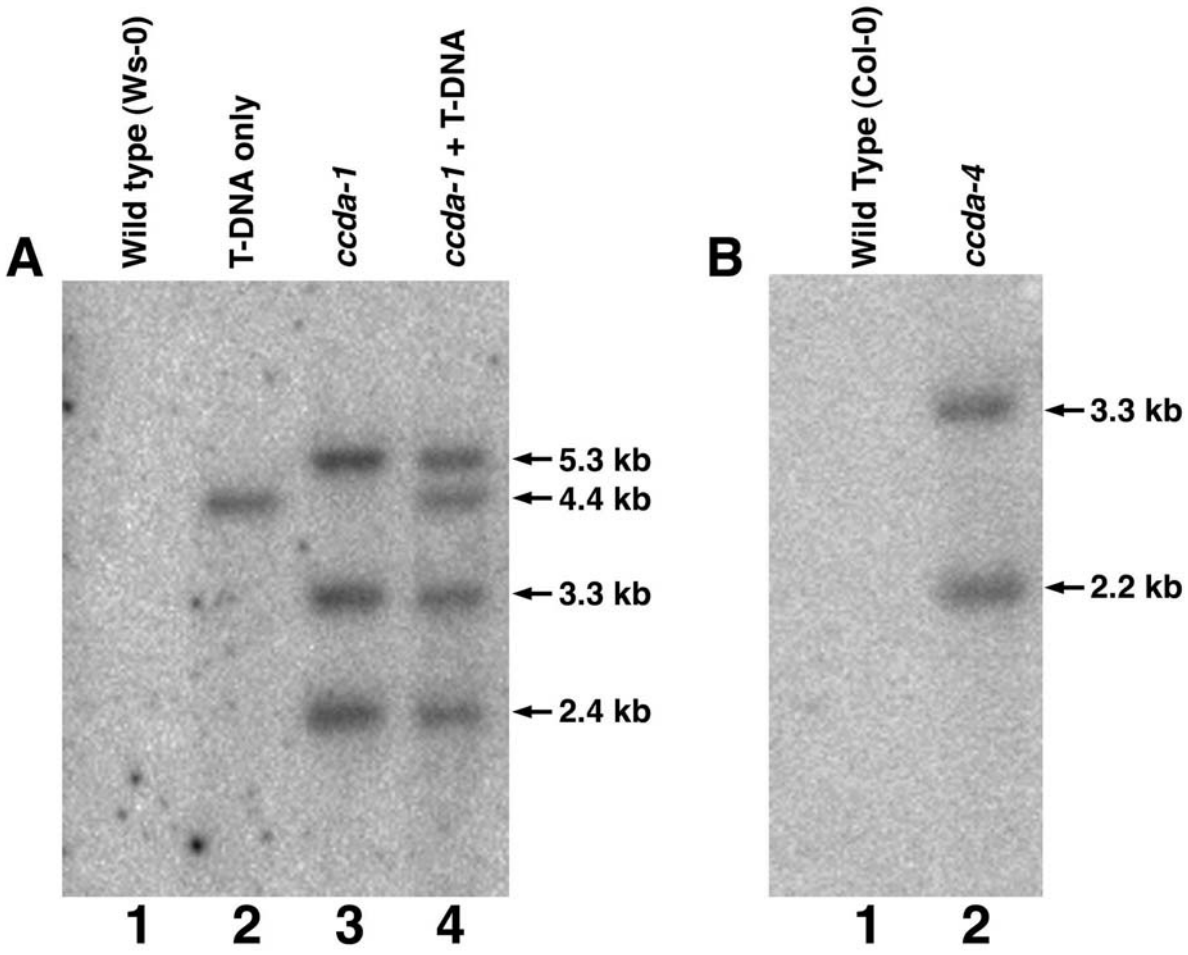
A
Wild type (Ws-0)
T-DNA only
ccda-1
ccda-1 + T-DNA
5.3 kb
4.4 kb
3.3 kb
2.4 kb
1
2
3
4
B
Wild Type (Col-0)
ccda-4
3.3 kb
2.2 kb
1
2

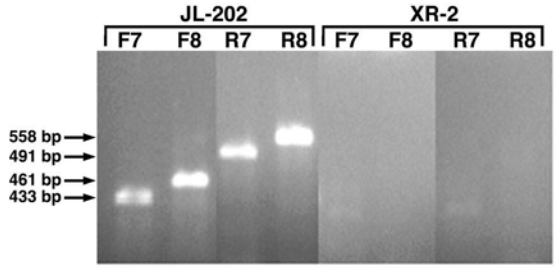

ccda-1

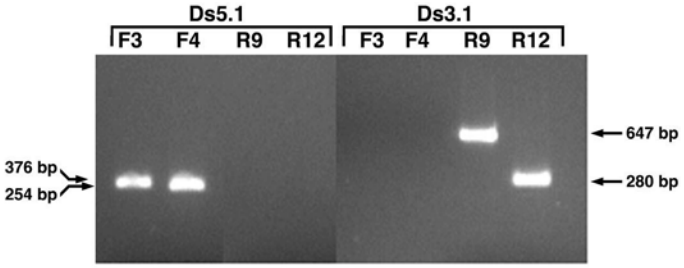

ccda-2

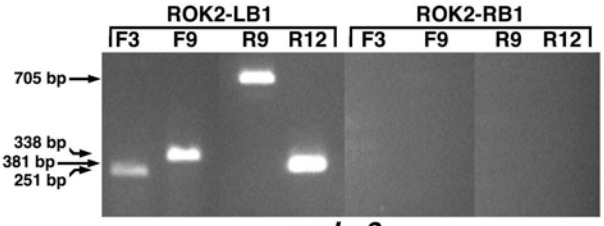

ccda-3

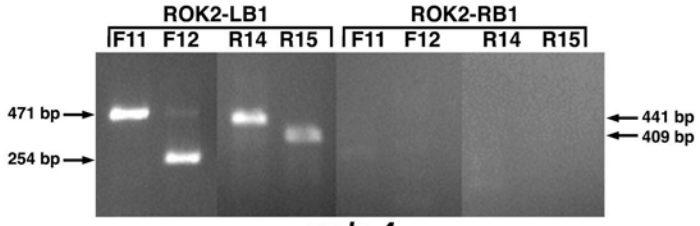

ccda-4